5-29-1965

A Theoretical Study Of Light Scattering From Water Droplets.

Aaron J. Cox

A THEORETICAL STUDY OF LIGHT SCATTERING FROM WATER DROPLETS

By

Aaron J. Cox, Jr.

A Thesis

Submitted in Partial Fulfillment of the

Requirements for the Degree of

Master of Science in Physics

The University of New Mexico

1965

This thesis, directed and approved by the candidate's committee, has been accepted by the Graduate Committee of the University of New Mexico in partial fulfillment of the requirements for the degree of

MASTER OF SCIENCE

H J Hendrickson
Dean

5/24/65
Date

A THEORETICAL STUDY OF LIGHT SCATTERING FROM WATER DROPLETS

Aaron J. Cox, Jr.

Thesis committee

Howard C. Bryant
Chairman

J L Howarth

Christopher Dean

TABLE OF CONTENTS

ACKNOWLEDGEMENTS

I would like to thank Dr. H.C. Bryant for his helpful advice and encouragement on the theoretical aspects of this paper. Also, I wish to thank Mr. D.B. Hayes, Mr. D.F. Warnke and Miss C. Tinsmith for their assistance on the computer work.

LIST OF GRAPHS

LIST OF ILLUSTRATIONS

INTRODUCTION

If an individual were to stand in such a way that his shadow were cast upon a cloud or mist of water droplets, then he might observe a multicolored halo about the shadow of his head. Such a phenomenon is often referred to as "the glory." There are numerous historical records of its observation in just such a manner. From the relative positions of the observer and his shadow on the cloud, it is apparent that the glory is in some way related to the backscattering of light from the individual droplets of which the cloud is composed.

In this paper an investigation of the scattering process itself is made. Special consideration is given to the behavior of the light scattered from a single droplet in directions at or near the backscattering angle. Extensive numerical calculations are made, based almost entirely upon the work of Gustav Mie.[1] Mie's work consisted of calculating the electromagnetic fields due to the scattering of a plane wave incident on a spherical particle in a homogeneous medium. It is hoped that these calculations will suggest a backscattering mechanism which will bridge the apparent gap between the exact, but rather involved, solution of Mie and the simpler approach of geometrical optics.

---

[1] G. Mie, Annalen Der Physik, Volumn 25, 1908, p. 377.

The difficulty arises in that for backscattering from water droplets geometrical optics seems to fail completely. The Mie solution is indeed exact but does not separate out the possible scattering mechanisms such as reflection, refraction and diffraction. Instead, all of these phenomena are included within the boundary value solution, and it is difficult to determine the contribution of each of these effects to the observed scattering. In this paper such a determination is attempted.

GENERAL THEORY

It shall now be our purpose to investigate, in some detail, the nature of light scattered from a spherical particle. In particular, we will be concerned with the case where a plane wave, traveling in a homogeneous, non-conducting medium, is incident on a single spherical particle. The particle may be composed of conducting or dielectric material.

Before going into the Mie treatment of this problem, which is the basis of all subsequent calculations, let us discuss briefly the general approach that will be taken.[2]

Consider a plane wave (with wave length λ) traveling in the positive z direction incident upon a particle of arbitrary shape. If this is a scalar wave or a single component of a vector wave it can be written as follows:

$$u_0 = e^{-ikz+i\omega t} \tag{2-1}$$

where $k = \frac{2\pi}{\lambda}$ and ω is the angular frequency of the vibration. After scattering has occurred we have an outgoing, spherical wave at a distance, r , from the drop which is large compared to the drop size and wave length of

---

[2]For completeness the entire Mie derivation and general theory has been included. The primary reference source has been H.C. Van de Hulst in Light Scattering by Small Particles (New York: John Wiley & Sons, 1957). His notation has been retained.

the incident wave. The amplitude of this wave is inversely proportional to r, and its angular distribution about the drop is governed by the so-called "amplitude function" or "scattering function," $S(\theta, \phi)$. The angles θ and ϕ are the normal spherical polar coordinates chosen such that θ is zero in the direction of $+Z$ and the origin is at the center of the drop. The reference for ϕ equal to zero is arbitrary at this point in the discussion. The scattered wave can thus be written in following form:

2-2 $$U = \frac{S(\theta, \phi)\, e^{-ikr + i\omega t}}{ikr}$$

Note that we have added a factor of ik in the denominator. The i is for later convenience, and the $k = \frac{2\pi}{\lambda}$ allows $S(\theta, \phi)$ to be a dimensionless number. It is now possible to write the scattered wave as a function of the incident wave.

2-3 $$U = \frac{S(\theta, \phi)\, e^{-ikr + ikz}}{ikr} U_0$$

In order to know the intensity of the light as a function of spatial position, we merely square the amplitude and have

2-4 $$I = \frac{S^2(\theta, \phi)}{k^2 r^2} I_0$$ (scattered intensity)

Where I_0 is the intensity of the incident plane wave in units of energy per unit time per unit area. This is called irradiance in optics.

We are primarily concerned with the effects of the presence of the scattering particle on the incident beam. In general, two things can occur:

(1) The wave can be scattered in all directions about the scattering center.

(2) Part of the wave can be absorbed through possible conduction within the particle itself.

The first of these is described by the scattering cross section, σ_{scat} . The second is described by the absorption cross section σ_{abs} . Both of these effects tend to remove light from the primary beam, and therefore combine to express the ability of the particle to detract from the original plane wave. This combination is called the "extinction cross section," σ_{ext} . Energy conservation then gives

2-5 $$\sigma_{ext} = \sigma_{scat} + \sigma_{abs} .$$

This paper will be concerned with scattering from water droplets with negligible conductivity, i.e., no absorption. Therefore:

2-6 $$\sigma_{ext} = \sigma_{scat}$$

Another feature of the single particle scattering theory, as will be developed here, is that it can be easily extended to many particles distributed randomly in an otherwise homogeneous medium. The only conditions that must be imposed on this extension are: first, that the particles be randomly distributed and second, that they be separated by a distance that is large with respect to the wave length of the light.

The formalities of this extension begin by considering many particles distributed throughout a homogeneous medium

as described above. These particles are not necessarily alike in size and shape. Each one will then have its own scattering function $S(\theta, \phi)$. Since they are separated by distances which are randomly distributed, and large with respect to the wave length, the phase relationships of the scattered light from different particles would be of a random nature also, changing very rapidly with time during one observation. For this reason we add the intensity of the scattered light from each particle without regard to phase, rather than the individual amplitudes, when computing the scattered intensity of a cloud of particles.

Thus far we have been discussing the scattering of scalar waves. However, we wish to extend the analysis to polarized light and to be able to describe the polarization effects which result from the scattering process itself. This requires the replacement of the scalar scattering function, $S(\theta, \phi)$, by a four by four matrix, $\mathcal{S}(\theta, \phi)$ where

2-7 $$\mathcal{S}(\theta, \phi) = \begin{pmatrix} S_2(\theta, \phi) & S_3(\theta, \phi) \\ S_4(\theta, \phi) & S_1(\theta, \phi) \end{pmatrix}$$

Such a replacement will allow the simultaneous treatment of the two polarization vectors of the electric field, $\vec{E}_{\parallel}$ and $\vec{E}_{\perp}$, where these refer to the components of the electric field which are parallel and perpendicular respectively to the scattering plane (see Fig. #1). Using this convention

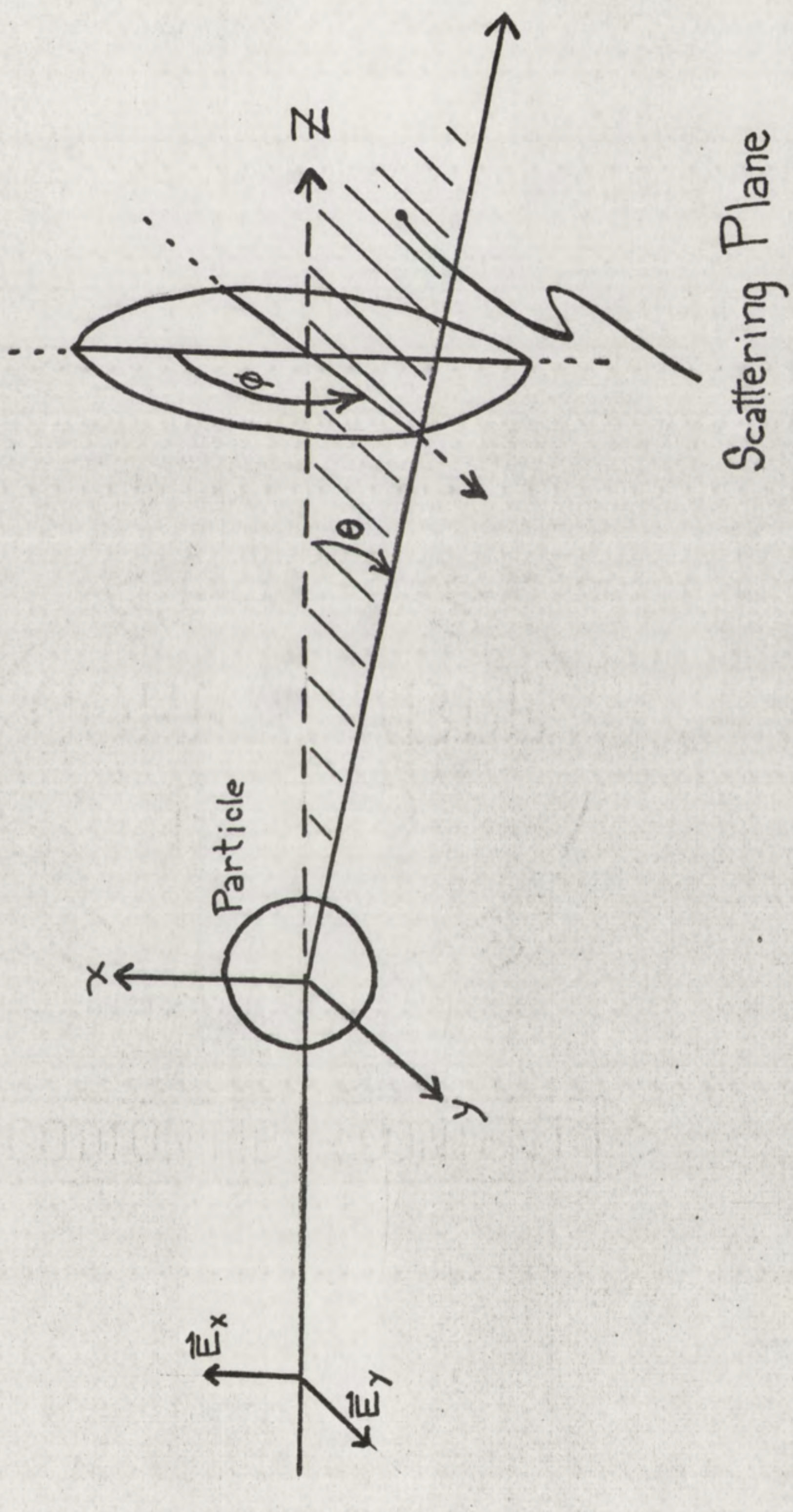

Figure 1.

equation 2-3 can be rewritten as a matrix equation containing both polarization directions.

$$\begin{pmatrix} E_{\parallel} \\ E_{\perp} \end{pmatrix} = S \cdot \frac{e^{-ikr+ikz}}{ikr} \begin{pmatrix} E_{\parallel_0} \\ E_{\perp_0} \end{pmatrix} \qquad \text{2-8}$$

The Mie theory treats only the case of spherical particles. This restriction greatly simplifies the above equation. First the elements S_3 and S_4 are equal to zero. Second, the remaining elements are functions of Θ only. These conditions thus allow equation 2-8 to be written as two scalar equations:

$$E_{\perp} = \frac{S_1(\theta)\, e^{-ikr+i\omega t}}{ikr} E_{\perp_0}$$

$$E_{\parallel} = S_2(\theta)\frac{e^{-ikr+i\omega t}}{ikr} E_{\parallel_0} \qquad \text{2-9}$$

The scattered intensities may now be written as functions of the polarization of the incident light, its wavelength, the radial distance from the drop and the angle θ. The intensities are dependent on the "intensity functions," $I1$ and $I2$. These functions are given by

$$I1 = |S_1(\theta)|^2 \qquad I2 = |S_2(\theta)|^2$$

For plane polarized light perpendicular to the scattering plane, with intensity I_0 we have

$$I = \frac{I1}{k^2 r^2} I_0 \qquad \text{2-10}$$

With polarization parallel to the scattering plane we would have a scattering intensity given by

2-11 $$I = \frac{I2}{k^2 r^2} I_0$$

Unpolarized or natural light would have an intensity of

2-12 $$I = \frac{(I1 + I2)}{2 k^2 r^2} I_0$$

It is apparent that if we can calculate the two complex scattering functions, $S_1(\theta)$ and $S_2(\theta)$, the nature of the scattered light can be described in great detail.

THE MIE SOLUTION

In order to calculate these quantities we must consider the electromagnetic character of light itself. This requires that Maxwell's equations be satisfied.[3] They are:

3-1 $$\operatorname{curl} \vec{H} = \frac{4\pi \vec{I}}{c} + \frac{1}{c}\frac{d\vec{D}}{dt}$$

3-2 $$\operatorname{curl} \vec{E} = -\frac{1}{c}\frac{d\vec{H}}{dt}$$

where $\vec{D} = \varepsilon E$ and $\vec{I} = \sigma \vec{E}$. In the above expressions we have: $\vec{H}$ — magnetic field strength, $\vec{E}$ — electric field strength, $\vec{D}$ — dielectric displacement, $\vec{I}$ — current density, ε — dielectric constant, σ — conductivity, t — time, and c — velocity of light. Using these variables the charge conservation equation takes the following form:

3-3 $$\operatorname{div} \vec{I} + \frac{d\rho}{dt} = 0$$

If we take the divergence of equation 3-1 we have

3-4 $$4\pi \operatorname{div} \vec{I} + \frac{d}{dt}\operatorname{div}\vec{D} = 0$$

Substituting equation 3-3 we have

$$4\pi \frac{d\rho}{dt} = \frac{d}{dt}\operatorname{div}\vec{D}$$

---

[3] Gaussian units will be used throughout this paper.

Assuming this equation to be valid at all times, t , we then write:

3-5 $$\operatorname{div} \vec{D} = 4\pi\rho$$

The divergence of equation 3-2 yields:

3-6 $$\operatorname{div} \vec{H} = 0$$

These are the equations that we will be using throughout the solution to the scattering problem. In the case of light waves we have time varying fields and they will be assumed to have the periodic behavior

3-7 $$A(t) = (\alpha + i\beta)\, e^{i\omega t}$$

Using this form the two Maxwell equations, 3-1 and 3-2, take on the form[4]

3-8 $$\operatorname{curl} \vec{H} = ikm^2 \vec{E}$$

3-9 $$\operatorname{curl} \vec{E} = -ik \vec{H}$$

where

$$k = \frac{\omega}{c} = \frac{2\pi}{\lambda} \quad \text{and} \quad m^2 = \mathcal{E} - \frac{4\pi i \sigma}{\omega}$$

In the above expressions, m is the complex index of refraction of the medium in which the light is traveling and k is the propagation constant. Note that m is a function of ω, the angular frequency of the light wave.

If we take the divergence of equation 3-8 we have

3-10 $$\operatorname{div} (m^2 E) = 0$$

and if we have a homogeneous medium, i.e., $m =$ constant we

---

[4] See appendix I

can write:

3-11 $$\operatorname{div} \vec{E} = 0$$

Combining equations 3-8, 3-9,3-6 and 3-11 we find that both $\vec{H}$ and $\vec{E}$ satisfy the vector wave equation of the form

3-12 $$\nabla^2 \vec{A} + k^2 m^2 \vec{A} = 0$$

From this we can state that any rectangular component of $\vec{E}$ or $\vec{H}$ will satisfy the scalar wave equation

3-13 $$\nabla^2 \psi + k^2 m^2 \psi = 0$$

This has the simple plane wave solution given by

3-14 $$\psi = e^{ikz + i\omega t}$$

We now consider a plane wave, of unit amplitude, traveling in a homogeneous medium with refractive index equal to 1. It will be incident on a sphere with a refractive index m, and we wish to calculate the resultant electromagnetic field as a function of position about the sphere. First we must solve the above vector wave equation in the spherical coordinates, r, θ, ϕ. To do this we make use of the fact that if ψ is a solution to the scalar wave equation,

$$\nabla^2 \psi + k^2 m^2 \psi = 0$$

then $\vec{M}_\psi$ and $\vec{N}_\psi$ given by

3-15 $$\vec{M}_\psi = \operatorname{curl} (\vec{r} \psi)$$

3-16 $$\vec{N}_\psi = \frac{1}{mk} \operatorname{curl} \vec{M}_\psi$$

are two vector solutions to the vector wave equation.[6]

---

[5] See Appendix II

[6] P.M. Morse and H. Feshbach, Methods of Theoretical Physics (New York: McGraw-Hill Inc., 1953), p. 1762.

Also the two vectors $\vec{M}$, $\vec{N}$ are related as follows:

3-17 $$mk\vec{M}_\psi = \text{curl}\, N_\psi$$

These relations are sufficient to write the two vectors $\vec{E}$ and $\vec{H}$ in term of two solutions u , v to the scalar wave equation. They are

3-18 $$\vec{E} = \vec{M}_v + i\vec{N}_u$$

3-19 $$\vec{H} = m(i\vec{N}_v - \vec{M}_u)$$

where $\vec{M}_v$; $\vec{M}_u$, $\vec{N}_v$, $\vec{N}_u$ are vectors derived from u and v using equations 3-15 and 3-16.[7]

Now consider the electromagnetic plane wave which is linearly polarized, having the following $\vec{E}$, and $\vec{H}$ vectors:

3-20 $$\vec{E} = \vec{a}_x e^{-ikz+i\omega t}$$
$$\vec{H} = \vec{a}_y e^{-ikz+i\omega t}$$

where $\vec{a}_x$, and $\vec{a}_y$ are unit vectors along the x and y axis respectively.

We write the solutions to the scalar wave equation, which are scalar plane waves, in spherical coordinates

$$u = e^{i\omega t} \cos\phi \sum_{n=1}^{\infty} (-1)^n \frac{2n+1}{n(n+1)} P_n^1(\cos\theta)\, J_n(kr)$$

3-21 $$v = e^{i\omega t} \sin\phi \sum_{n=1}^{\infty} (-1)^n \frac{2n+1}{n(n+1)} P_n^1(\cos\theta)\, J_n(kr)$$
(Incident Plane Waves)

where $P_n^1(\cos\theta)$ is an associated Legendre polynomial and $J_n(kr)$ is a spherical Bessel function of order n .[8]

Our final solution will be the sum of an incident plane wave and a scattered spherical wave. At infinity we will

---

[7]See Appendix III.

[8]R.M. Eisberg, Fundamentals of Modern Physics (New York: John Wiley & Sons, 1961), p. 538.

have only the plane wave remaining, so we must have the spherical wave going to zero at infinity. This dictates the form which the scattered wave must take.

Outside Scattered Wave:

3-22
$$U = e^{i\omega t} \cos\phi \sum_{n=1}^{\infty} -a_n \frac{2n+1}{n(n+1)} P_n^1(\cos\theta)\, h_n(kr)$$
$$V = e^{i\omega t} \sin\phi \sum_{n=1}^{\infty} -b_n \frac{2n+1}{n(n+1)} P_n^1(\cos\theta)\, h_n(kr)$$

Here we use the spherical Bessel functions of the second kind, $h_n(kr)$, which have the needed asymptotic behavior as $r \to \infty$. That is

$$h_n(kr) \to i^{n+1} \frac{e^{-ikr}}{kr} \qquad \text{as } r \to \infty .$$

Inside the sphere we have another form.

Inside:

3-23
$$U = e^{i\omega t} \cos\phi \sum_{n=1}^{\infty} m c_n (-i)^n \frac{2n+1}{n(n+1)} P_n^1(\cos\theta)\, J_n(mkr)$$
$$V = e^{i\omega t} \sin\phi \sum_{n=1}^{\infty} m d_n (-i)^n \frac{2n+1}{n(n+1)} P_n^1(\cos\theta)\, J_n(mkr)$$

Note that we have added the factor of m (refractive index) since we are in the medium of the sphere. We have a_n, b_n, c_n, d_n as unknown coefficients to be determined. These are found by satisfying the electromagnetic boundary conditions at the surface of the sphere.

These conditions require: first, that tangential components of $\vec{E}$ and $\vec{H}$ be continuous.

That is: $$\vec{n} \times (\vec{H}_2 - \vec{H}_1) = 0$$

and

$$\vec{n} \times (\vec{E}_2 - \vec{E}_1) = 0$$

where

$\vec{n} \sim$ outward unit normal, $\vec{H}_2$, $\vec{H}_1$, and $\vec{E}_2, \vec{E}_1$ are the $\vec{H}$ and $\vec{E}$ vectors inside and outside the sphere respectively.

The normal components have the following conditions:

$$\vec{n} \cdot (m_2^2 \vec{E}_2 - m_1^2 \vec{E}_1) = 0$$

and

$$\vec{n} \cdot (\vec{H}_2 - \vec{H}_1) = 0$$

From equations 3-15 to 3-19 the θ and ϕ components of $\vec{E}$ and $\vec{H}$ can be obtained. They are

3-24 $$E_\theta = \frac{1}{r \sin\theta} \frac{\partial(rv)}{\partial\phi} + \frac{i}{mkr} \frac{\partial^2(ru)}{\partial r \partial\theta}$$

3-25 $$E_\phi = \frac{-1}{r} \frac{\partial(rv)}{\partial\theta} + \frac{i}{mkr \sin\theta} \frac{\partial^2(ru)}{\partial r \partial\phi}$$

3-26 $$H_\theta = \frac{i}{kr} \frac{\partial^2(rv)}{\partial r \partial\theta} + \frac{im}{r \sin\theta} \frac{\partial(ru)}{\partial\phi}$$

3-27 $$H_\phi = \frac{i}{kr \sin\theta} \frac{\partial^2(rv)}{\partial r \partial\phi} + \frac{im}{r} \frac{\partial(ru)}{\partial\theta}$$

The above components must be continuous at the surface of the sphere. Continuity of v and $\frac{\partial ru}{m \partial r}$ will insure that E_θ and E_ϕ are continuous across the surface. H_θ and H_ϕ will be continuous if mu and $\frac{\partial(rv)}{\partial r}$ are continuous across the surface. The indicated continuity conditions yield the

following set of equations: (m=1 in surrounding medium and m=m in sphere)

Continuity of mu :

3-28 $$m\, j_n(kr) - a_n\, m\, h_n(kr) = m^2 C_n j_n(mkr)$$

Continuity of $\frac{1}{m}\frac{\partial(ru)}{\partial r}$:

3-29 $$j_n(ka) + ka\, j_n'(ka) - a_n(h_n(ka) + ka\, h_n'(ka)) = C_n j_n(mka) + mka\, C_n j_n(mka)$$

Continuity of v:

3-30 $$j_n(ka) - b_n h_n(ka) = m\, d_n j_n(mka)$$

Continuity of $\frac{\partial(rv)}{\partial r}$:

3-31 $$ak\, j_n'(ka) + j_n(ka) - b_n ak\, h_n'(ka) - b_n h_n(ka) = d_n m^2 ka\, j_n(mka) + m d_n\, j_n(mka)$$

Defining two new functions, $\psi(x)$ and $\zeta_n(y)$, of the variables x and y where

$$\psi_n(x) = x\, j_n(x)$$

$$\zeta_n(y) = y\, h_n(y)$$

and

$$x = \frac{2\pi a}{\lambda}$$

$$y = mka$$

the four continuity equations become

3-32 mu : $$\psi_n(x) - a_n \zeta_n(x) = m\, C_n \psi_n(y)$$

3-33

$\frac{\partial(ru)}{m\partial r}$: $$\psi_n'(x) - a_n \zeta_n'(x) = C_n\, \psi_n'(y)$$

3-34 $$v:\quad \psi_n(x) - b_n\zeta_n'(x) = d_n\psi_n(y)$$

3-35 $$\frac{\partial(rv)}{\partial r}:\quad \psi_n'(x) - b_n\zeta_n'(x) = m d_n \psi_n'(y)$$

a_n, b_n, c_n and d_n can now be determined, since we have four equations and four unknowns. They have the values

3-36 $$a_n = \frac{\psi_n'(y)\,\psi_n(x) - m\,\psi_n(y)\,\psi_n'(x)}{\psi_n'(y)\zeta_n(x) - m\,\psi_n(y)\,\zeta_n(x)}$$

3-37 $$b_n = \frac{m\,\psi_n'(y)\,\psi_n(x) - \psi_n(y)\,\psi_n'(x)}{m\,\psi_n'(y)\zeta_n(x) - \psi_n(y)\,\zeta_n'(x)}$$

3-38 $$c_n = \frac{i}{\psi_n'(y)\zeta_n(x) - m\,\psi_n(y)\zeta_n(x)}$$

3-39 $$d_n = \frac{i}{m\,\psi_n'(y)\,\zeta_n(x) - \psi_n(y)\,\zeta_n'(x)}$$

These are called the Mie coefficients.

The asymptotic form for $h_n(kr)$ is now substituted in the equations for the two scattered waves u and v. They become

3-40 $$u = \frac{-i}{kr}\,e^{-ikr+i\omega t}\cos\phi \sum_{n=1}^{\infty} a_n \frac{2n+1}{n(n+1)} P_n^1(\cos\theta)$$

3-41 $$V = \frac{-i}{kr} e^{-ikr+i\omega t} \sin\phi \sum_{n=1}^{\infty} b_n \frac{2n+1}{n(n+1)} P_n^1(\cos\theta)$$

From equations 3-15 through 3-19 the tangential field components can be obtained.[9] They are

3-42 $$E_\theta = H_\phi = \frac{-i}{kr} e^{ikr+i\omega t} \cos\phi \; S_2(\theta)$$

3-43 $$-E_\phi = H_\theta = \frac{-i}{kr} e^{-ikr+i\omega t} \sin\phi \; S_1(\theta)$$

where

$$S_1(\theta) = \sum_{n=1}^{\infty} \frac{2n+1}{n(n+1)} \left\{ a_n \pi_n(\theta) + b_n \tau_n(\theta) \right\}$$

$$S_2(\theta) = \sum_{n=1}^{\infty} \frac{2n+1}{n(n+1)} \left\{ b_n \pi_n(\theta) + a_n \tau_n(\theta) \right\}$$

and

$$\pi_n(\theta) = \frac{1}{\sin\theta} P_n^1(\cos\theta)$$

$$\tau_n(\theta) = \frac{d}{d\theta} P_n^1(\cos\theta)$$

---

[9]See Appendix IV.

The functions $S_1(\theta)$ and $S_2(\theta)$ are the so-called scattering functions mentioned earlier in this section, since the perpendicular and parallel components of the incident electric field are

3-44 $$E_{\perp} = \sin \phi$$

3-45 $$E_{\parallel} = \cos \phi$$

The scattered field is

3-46 $$E_{\perp} = -E_{\phi}$$

3-47 $$E_{\parallel} = E_{\theta}$$

The expressions for the scattering functions have been found. Scattered intensities at various angular positions around the drop may now be calculated.

THE PROGRAMS

In order to study in numerical detail the characteristics of light scattered by dielectric spheres (in this case water droplets) several computer programs were written. The following properties of the scattered light were to be investigated:

(a) Convergence of the series describing the intensities of the two polarization directions.

i.e.,
$$I1 = \left| \sum_{n=1}^{\infty} (a_n \pi_n + b_n \tau_n) \right|^2$$
$$I2 = \left| \sum_{n=1}^{\infty} (a_n \tau_n + b_n \pi_n) \right|^2$$

(b) Dependence of $I1$, $I2$, σ_{ext} (total cross section) on drop size.

(c) Angular dependence of $I1$, $I2$.

The first task, then, was to generate a complete series of Mie coefficients which would be functions of λ (wavelength) a (drop radius) and m (index of refraction).[10] This in turn required the generation of Ricatti-Bessel functions, and their derivatives evaluated for real and complex arguments due to the complex nature of m. Since water was of primary interest as a scattering material, and its index of refraction has a negligably small imaginary part, the original program was written to accommodate only real <u>refractive</u> <u>indices</u>.

---

[10] The "completeness" of such a series was actually a subject of investigation as it is dependent upon the convergence of the series itself.

The Ricatti-Bessel functions are related to the common spherical Bessel functions as follows:

4-1 $$\psi_n(z) = z\,j_n(z) = \left(\frac{\pi z}{2}\right)^{1/2} J_{n+1/2}(z)$$

4-2 $$\chi_n(z) = -z\,n_n(z) = -\left(\frac{\pi z}{2}\right)^{1/2} N_{n+1/2}(z)$$

4-3 $$\zeta_n(z) = \psi_n(z) + i\chi_n(z)$$

Where $J_{n+1/2}(z)$ is an ordinary Bessel function of half integer order and $j_n(z)$ is the ordinary spherical Bessel function. $N_{n+1/2}(z)$ is the Neuman function of half integer order. These functions were evaluated for a given argument and order as needed in the relations for a_n and b_n. The order was advanced from $n=0$ up to some terminating value N which will be discussed later. To accomplish this the following recursion relations were used:

4-4 $$j_{n+1}(z) = \left(\frac{2n+1}{z}\right) j_n(z) - j_{n-1}(z)$$

and

4-5 $$\frac{d}{dz} j_n(z) = \frac{n}{(2n+1)} j_{n-1}(z) - \frac{(n+1)}{(2n+1)} j_{n+1}(z)$$

The series was started using $$j_0(z) = \frac{\sin z}{z}$$

and

4-6 $$j_{-1}(z) = \frac{\cos z}{z}$$

The function $n_n(z)$ is related to $j_n(z)$ by the relation

4-7 $$n_n(z) = j_{-n-1}(z)$$

and so the generation of $n_n(z)$ was accomplished by merely evaluating the spherical Bessel functions for negative order,

using the above recursion relations.

This program was used to study the convergence of the sequences of a_n and b_n, but was found to be rather slow in terms of machine running time; and a second program was written. In addition to being much quicker, the second program was capable of handling a scattering sphere with a complex index of refraction, i.e., a conducting sphere.

Following the work of D. Deirmendjian and R.J. Clasen the recursion relations for the Mie coefficients take a much simpler form:

4-8
$$a_n = \frac{\left(\frac{A_n}{m} + \frac{n}{x}\right) J_{n+\frac{1}{2}}(x) - J_{n-\frac{1}{2}}(x)}{\left(\frac{A_n}{m} + \frac{n}{x}\right)\left[J_{n+\frac{1}{2}}(x) + i(-1)^n J_{-n-\frac{1}{2}}(x)\right] - J_{n-\frac{1}{2}}(x) + (-i)^n J_{-n+\frac{1}{2}}(x)}$$

For b_n we replace $\frac{A_n}{m}$ by $m A_n$ wherever it appears. The quantity A_n is given by the relation

4-9
$$A_n(mx) = -\frac{n}{mx} + \frac{1}{\frac{n}{mx} - A_{n-1}(mx)}$$

where

4-10
$$A_0(mx) = \frac{J_{-\frac{1}{2}}(mx)}{J_{+\frac{1}{2}}(mx)} = \cot(mx)$$

The $J_{n+\frac{1}{2}}(x)$ and $J_{-n-\frac{1}{2}}(x)$ are, as before,

---

[11] D. Deirmendjian and R.J. Clasen, Light Scattering on Partially Absorbing Homogeneous Spheres of Finite Size, (Santa Monica: The Rand Corp., 1962), p. 4.

Bessel functions of half integer order. Note that except for the initial value for A_n, all of the Bessel functions are evaluated for real arguments only. This removes the problem encountered with the previous program where the Bessel functions had complex arguments whenever the refractive index was complex. These equations were then separated into real and imaginary parts. That is, a separate recursion relation was written for the real and the imaginary parts of a_n, b_n, A_n respectively. This allowed the use of double precision arithmetic within the computer. Using double precision arithmetic, 22 significant figures were carried for all computed quantities. This was done in order to minimize errors from loss of significant figures due to subtraction in the recursion relations. π_n and the τ_n also take on the quite simple form

4-11 $$\pi_n(\theta) = \frac{(2n-1)}{n-1}\pi_{n-1}(\theta)\cos\theta - \frac{n}{n-1}\pi_{n-2}(\theta)$$

4-12
$$\tau_n(\theta) = \cos\theta\left[\pi_n(\theta) - \pi_{n-2}(\theta)\right] - (2n-1)\sin^2\theta\,\pi_{n-1}(\theta) + \tau_{n-2}(\theta)$$

where $\pi_0(\theta) = 0$ $\qquad \tau_0(\theta) = 0$

$$\pi_1(\theta) = 1 \qquad \tau_1(\theta) = \cos\theta$$

$$\pi_2(\theta) = 3\cos\theta \qquad \tau_2(\theta) = 3(\cos^2\theta - \sin^2\theta)$$

Figure #2 is a flow diagram of the second program.

It should be noted here that there is some confusion among different authors concerning the form that the Mie coefficients take. That is, the a_n's and b_n's generated by the above relations are consistent with those from the Van de Hulst[12] equations but are related to the coefficients calculated by Gumprecht and Sliepcenich,[13] Lowan,[14] and Boll, Churchill, Chu and Leacock,[15] by

4-13 $$a_n = a_n(VH)\,(-1)^{n+1/2}$$

4-14 $$b_n = b_n(VH)\,(-1)^{n+3/2}$$

where $a_n(VH)$ and $b_n(VH)$ are the coefficients from the Van de Hulst equations and a_n and b_n are those appearing in the tables of the other individuals. This apparent inconsistency is due to the choice of the scattering angle, which appears in $\pi_n(\theta)$ and $\tau_n(\theta)$. Where Van de Hulst chooses θ to be the angle between the direction of scattering and the direction of incoming radiation, the others choose the supplement of θ. This introduces negative arguments in $\pi_n(\theta)$ and $\tau_n(\theta)$ which cancel out the above-mentioned factors. If one is consistent with a sign convention, no

---

[12]Van de Hulst, op. cit., p. 123.

[13]R.O. Gumprecht and C.M. Sliepcenich, Light-Scattering Functions for Spherical Particles (Ann Arbor: University of Michigan Press, 1951), p. 13.

[14]A.N. Lowan, Tables of Scattering Functions for Spherical Particles, Department of Commerce, National Bureau of Standards Applied Mathematics Series #4 (Washington: U.S. Government Printing Office, 1949), p. 4.

[15]Boll, Chu, Churchill, Leacock, Tables of Light Scattering Functions (Ann Arbor: University of Michigan Press, 1958), p. 12.

trouble will occur; however, when consulting the literature it is important to be aware of which convention is being employed and its effect on the coefficients thus calculated.

Deirmendjian discusses two criteria for termination of the summation process when calculating $S_1(\theta)$, $S_2(\theta)$.[16] Summation may stop either when

4-15 $$\frac{|a_n| + |b_n|}{n} < 10^{-14}$$

4-16 or when $n = 1.2x + 9$ where

n is the order of the last term in the summation. The programs being considered required that both conditions be satisfied before summation ceased. It will be shown that convergence was achieved in all cases considered.

The calculations were performed on CDC 1604 and CDC 3600 computers. The graphs were automatically plotted from magnetic tape. Comparisons were made between output from these programs and previously tabulated work by Lowan,[17] Boll, Chu, Churchill and Leacock,[18] Pendorff,[19] and Gumprecht and Sliepcevich.[20] In all cases agreement was complete.

---

[16] Deirmendjian and Clasen, op. cit., p. 6.

[17] Lowan, op. cit., p. 4.

[18] Boll, Chu, Churchill and Leacock, op.cit., p. 12

[19] R. Penndorf and B. Goldberg, New Tables of Mie Scattering Functions for Spherical Particles, Geophysical Research Papers Number 45, Geophysics Research Directorate, Air Force Cambridge Research Center, Air Research and Development Command, 1956, p. 5.

[20] Gumprecht and Sliepcevich, op. cit., p. 13.

FIGURE 2

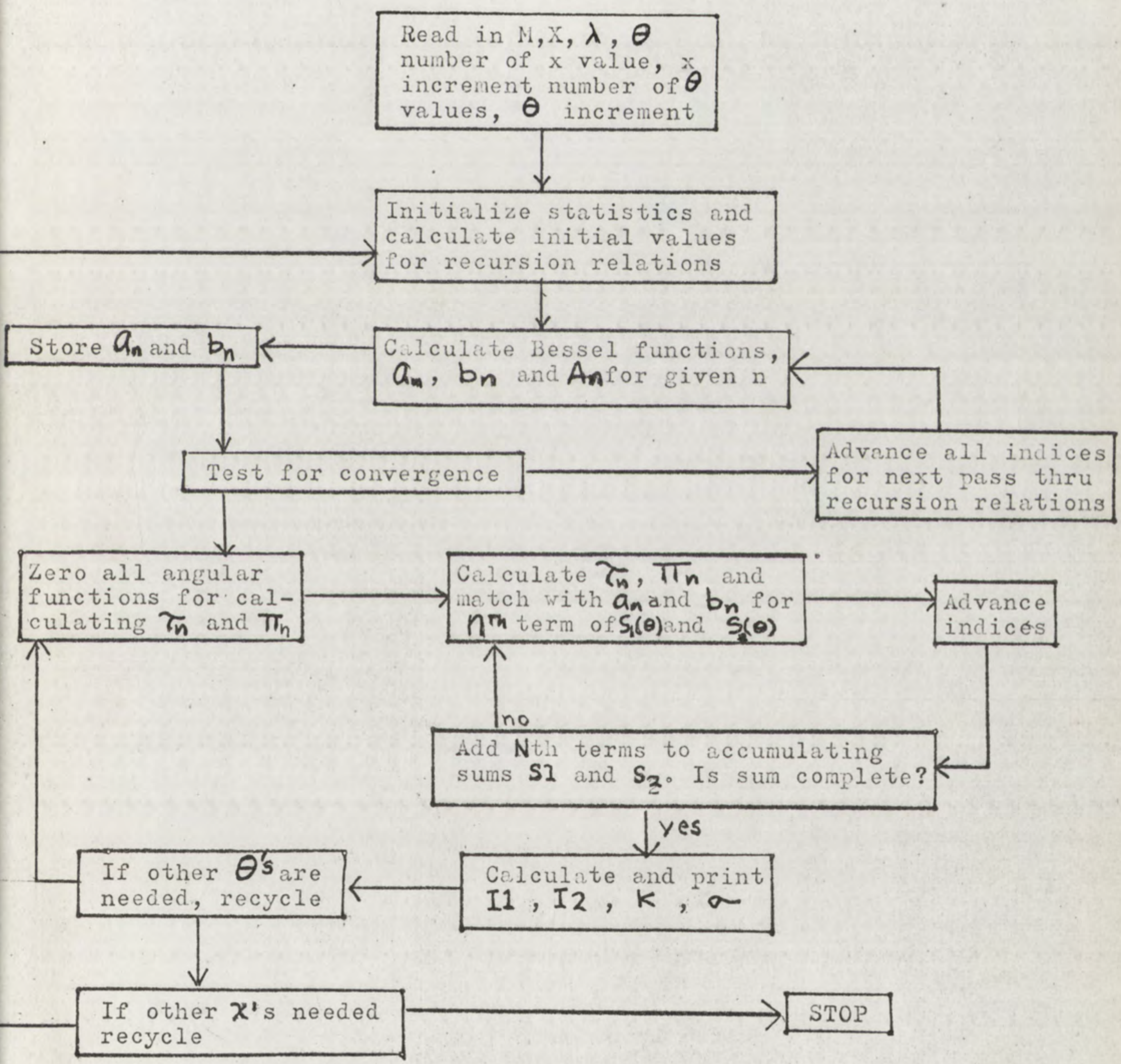
Read in M, X, λ, θ number of x value, x increment number of θ values, θ increment
Initialize statistics and calculate initial values for recursion relations
Store a_n and b_n
Calculate Bessel functions, a_m, b_n and A_n for given n
Test for convergence
Advance all indices for next pass thru recursion relations
Zero all angular functions for calculating τ_n and π_n
Calculate τ_n, π_n and match with a_n and b_n for n^{th} term of $S_1(\theta)$ and $S_2(\theta)$
Advance indices
no
Add Nth terms to accumulating sums S1 and S_2. Is sum complete?
yes
If other θ's are needed, recycle
Calculate and print I1, I2, k, σ
If other χ's needed recycle
STOP

RESULTS

The first calculations of $I1$ and $I2$ were made for water droplets with m equal to 1.3330 and θ equal to 180°. An initial value of 500.0 was chosen for x, and subsequent calculations were made at x intervals of 0.05 ($x = \frac{2\pi a}{\lambda}$ where a is the drop radius). This choice of intervals proved to be unsatisfactory, as interpolation was impossible. The interval was reduced to 0.005 and calculations were made at 400 x values beginning with 500. The results appear in Graph #1. The large fluctuations and their definite periodic character should be noted. As indicated on the graph, the peaks have periods of .815 in x.

The angular dependence of $I1$ and $I2$ was the next subject of investigation. Holding x fixed, calculations were made at 10° intervals between $\theta = 0°$ and $\theta = 180°$. Graph #2 illustrates the results. Again, the intervals were too large to permit interpolation. The data points were therefore connected with broken lines. Three peaks in the $I1$ curve are shown. The first, at $\theta = 0°$ is the very strong forward peak. The second, is shown at $\theta = 140°$. Geometrical optics predicts a peak at $\theta = 138°$ (the angle at which the rainbow appears); however, calculations were made only at 10° intervals and $\theta = 138°$ was not included. The third peak occurs at $\theta = 180°$.

Graph #1.

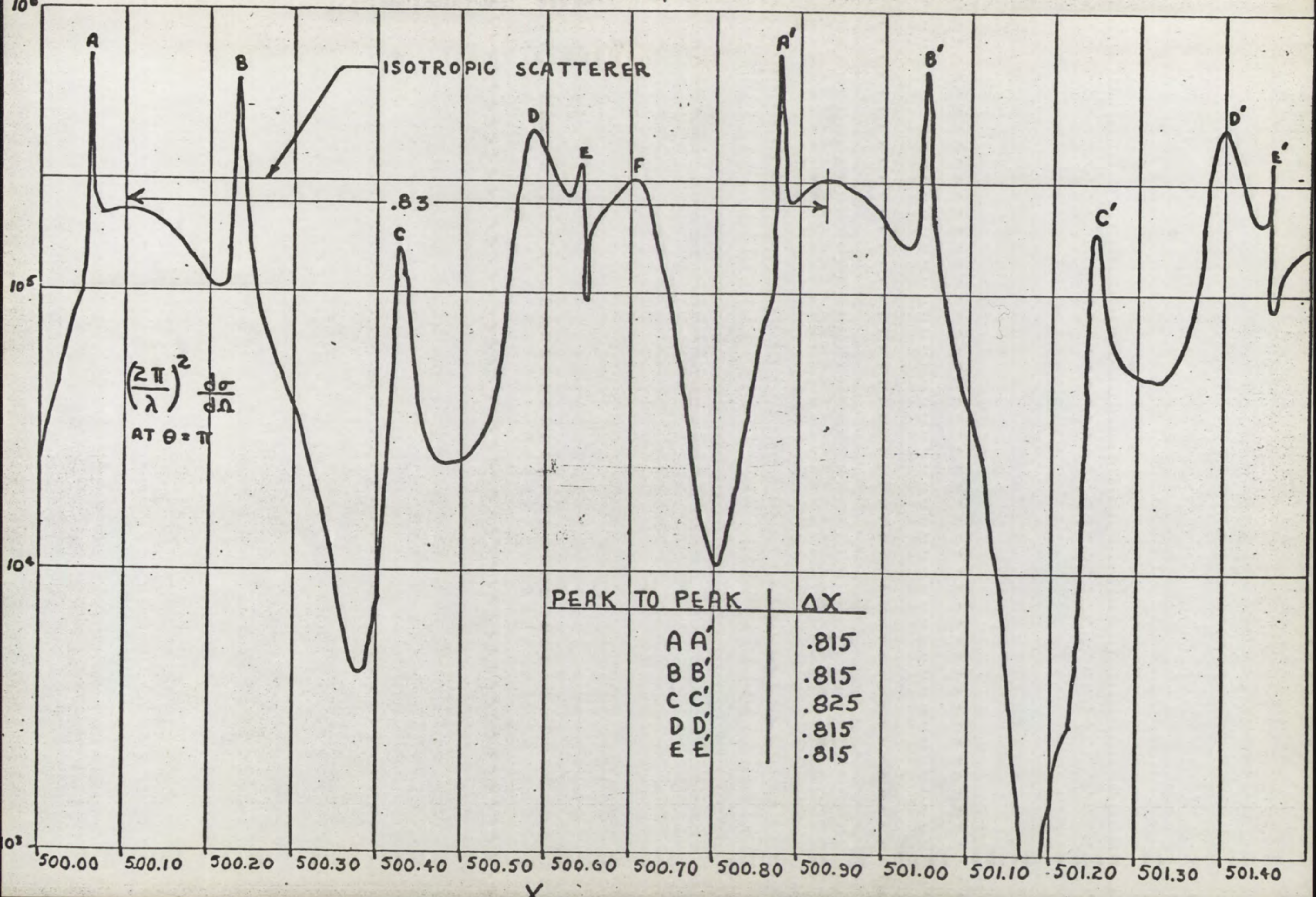

PEAK TO PEAK	ΔX
A A′	.815
B B′	.815
C C′	.825
D D′	.815
E E′	.815

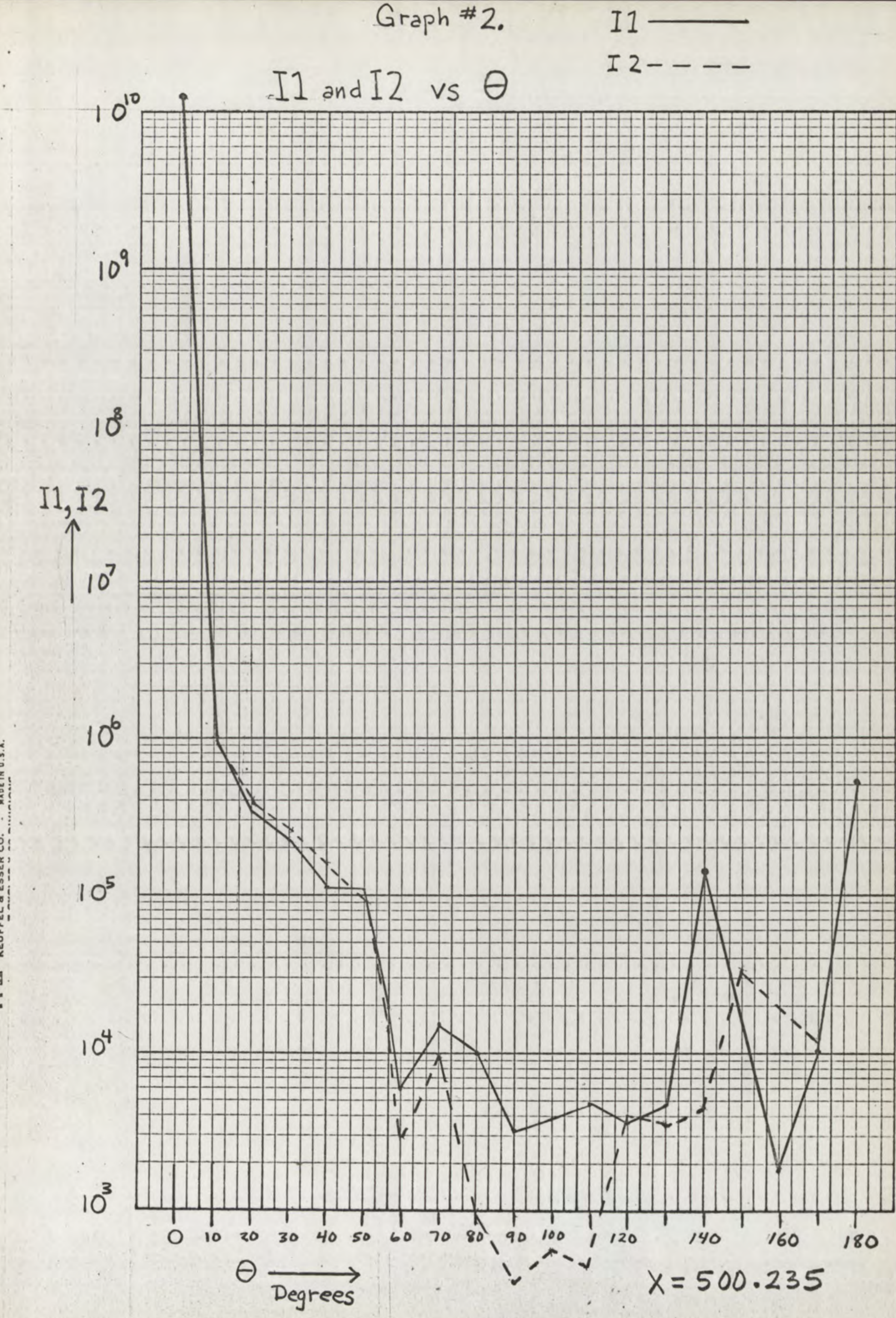
Graph #2.
I1 ———
I2 - - - -
I1 and I2 vs Θ
10^{10}
10^9
10^8
I1, I2
10^7
10^6
10^5
10^4
10^3
0
10
20
30
40
50
60
70
80
90
100
120
140
160
180
Θ
Degrees
X = 500.235
SEMI-LOGARITHMIC 359-96
KEUFFEL & ESSER CO. MADE IN U.S.A.

This is the angle at which glory is observed. At 0° and 180° I1 and I2 are equal.

To study the behavior of I1 and I2 in greater detail as θ approaches 180°, the angular increments were reduced to $.05^\circ$; and calculations were made for θ between 170° and 180°. I1 and I2 appear on Graph #3 and Graph #4 respectively. To compare I1 with I2 the envelope containing I1 has been superimposed on the I2 curve, clearly showing the predominance of I1 . This would indicate a preference for scattering light with polarization perpendicular to the scattering plane.

Returning to the χ dependence of the intensity functions, calculations were made for χ near 100, and $\theta = 180^\circ$, again using χ increments of .005. The results appear on the upper grid of Graph #5. The lower grid is a plot of the extinction coefficient, K as a function of χ, where

$$K = \frac{\sigma_{ext}}{\pi a^2}$$

For large drops K approaches a value of 2. The reason that the huge fluctuations in I1 are seen as very small ripples in the extinction coefficient is that K includes scattering over the entire solid angle of 4π steradians, whereas I1 is calculated for a single angular direction.

Next, the χ dependence of I1 and I2 was investigated at $\theta = 90^\circ$. The same set of χ values used on the previous calculation was chosen. Graphs #6a and #6b show the two intensity functions. The very high peaks seen on Graph #1 and

Graph #3.

I1 vs θ

I1

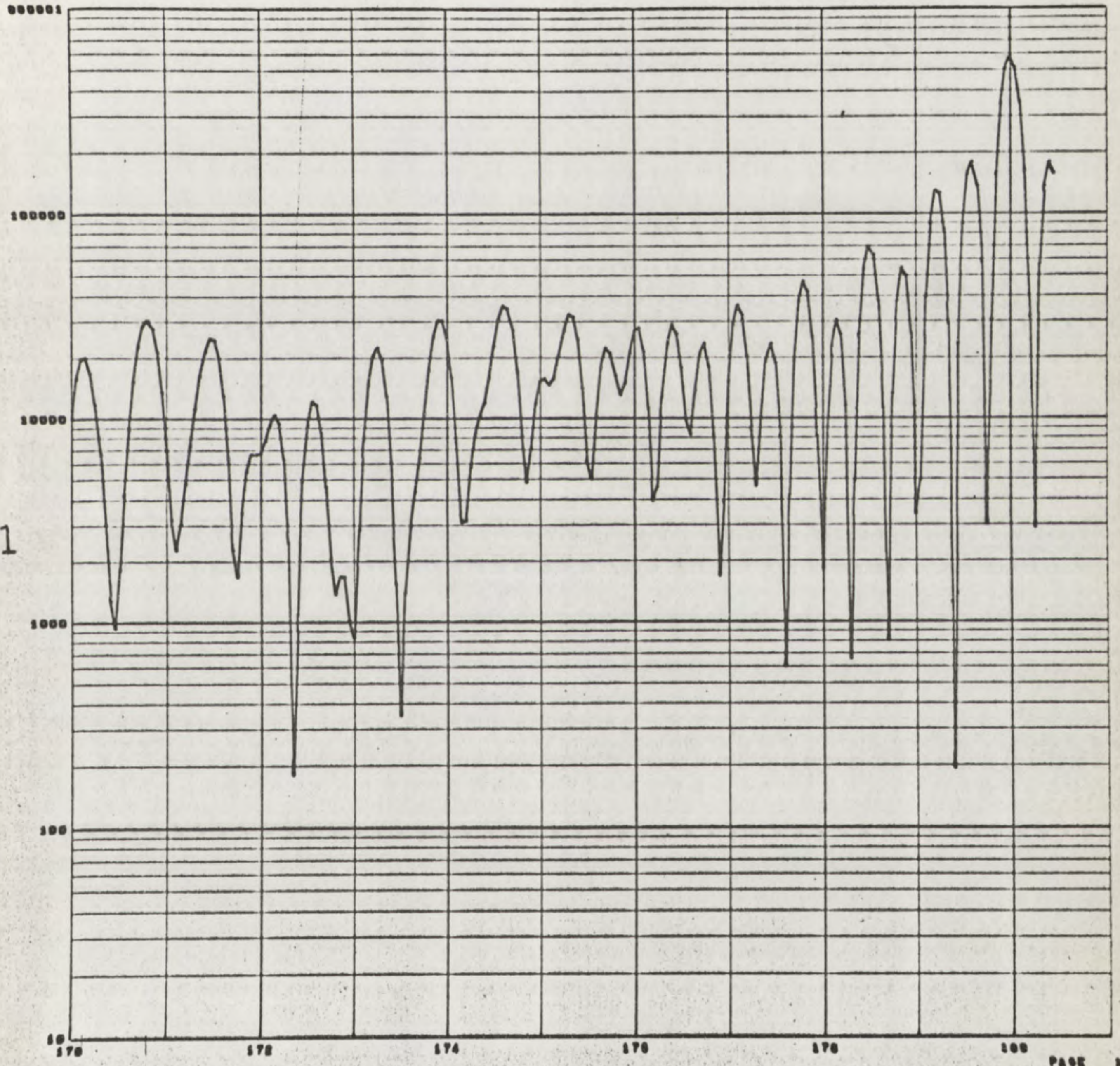

$\theta \longrightarrow$ Degrees

X = 500.235

Graph #4.

I2 vs θ

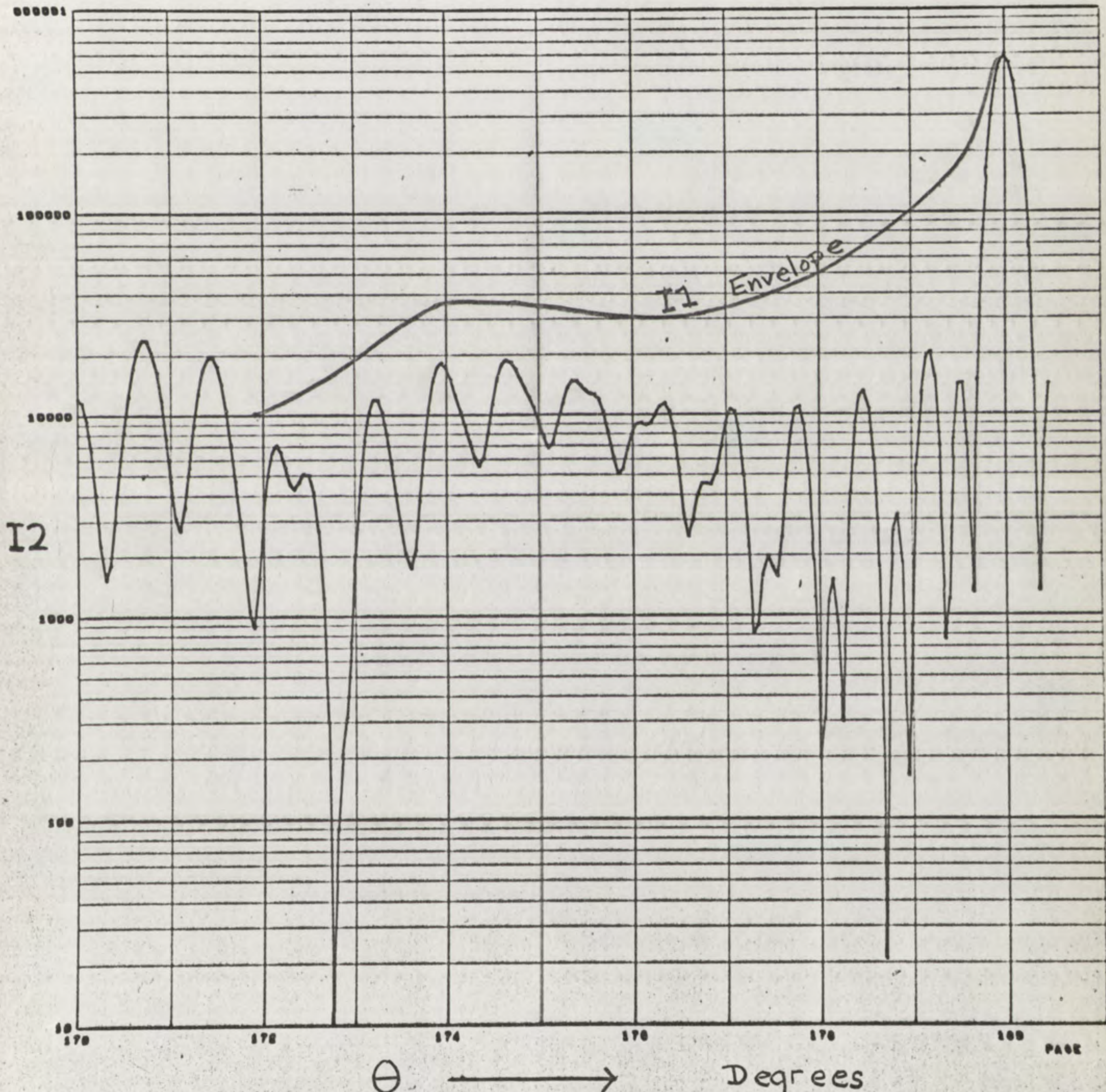

X = 500.235

Graph #5.

I1 and K vs. X or ALPHA

WATER - INDEX OF REFRACTION N= 1.333 THETA =180 X ≡ ALPHA

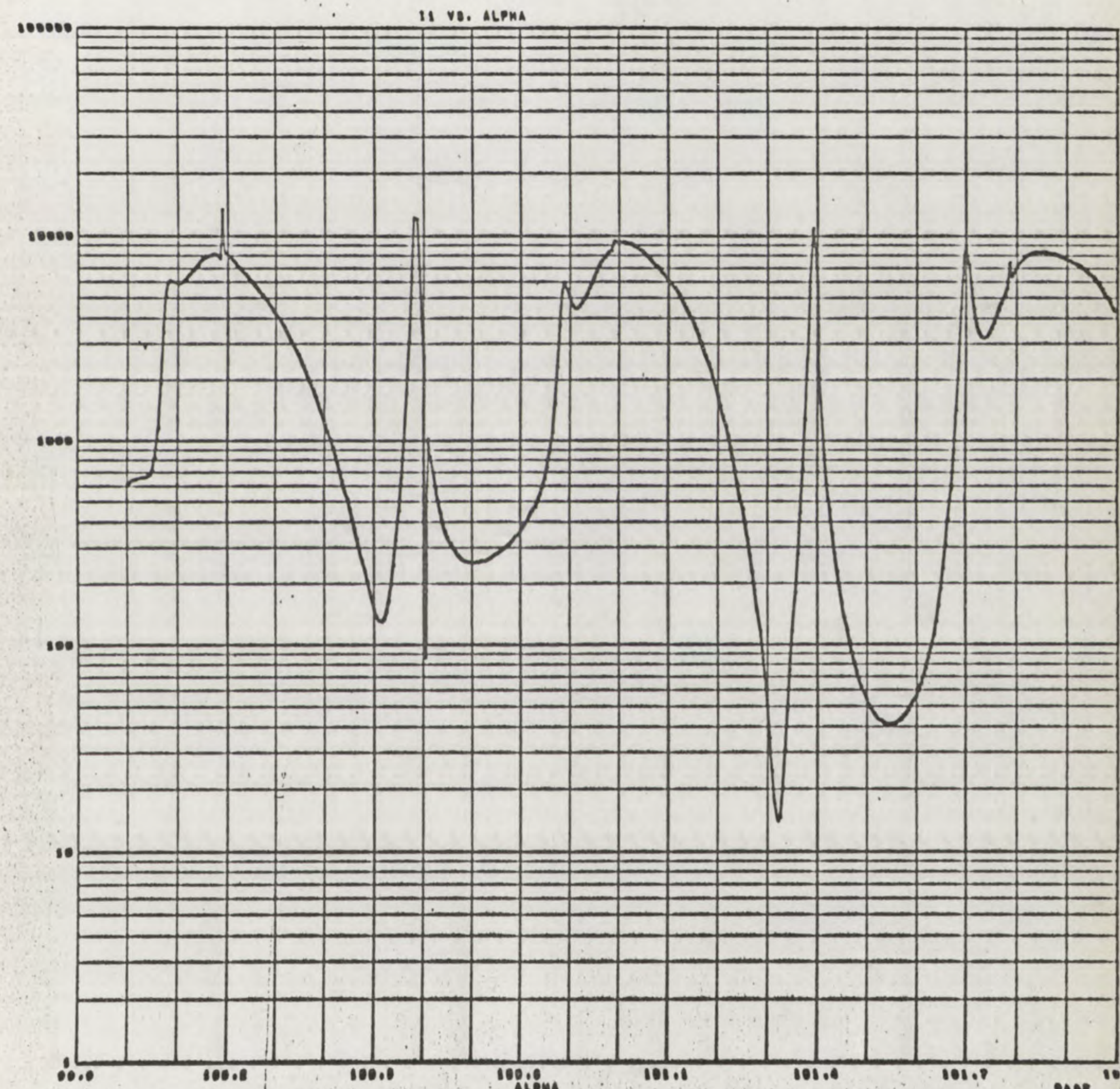

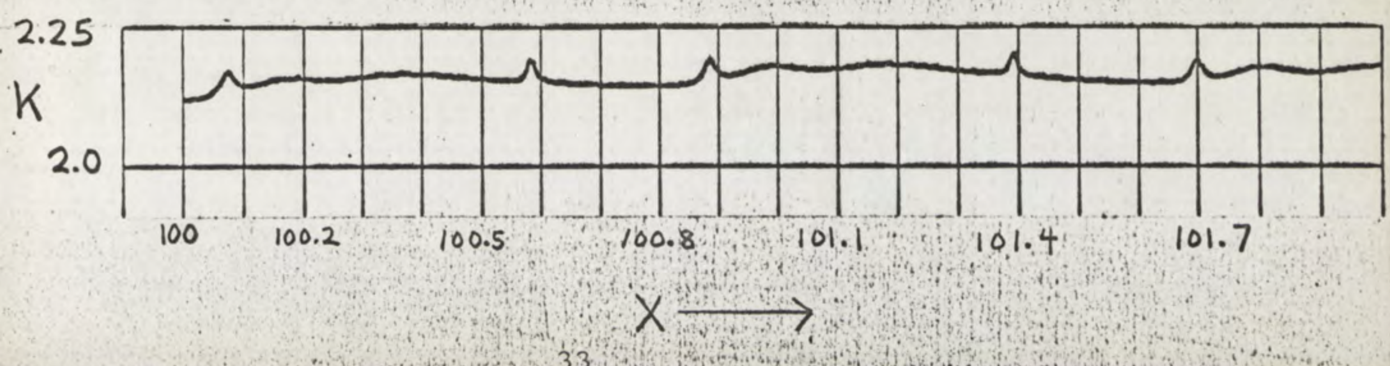

Graph #6a.

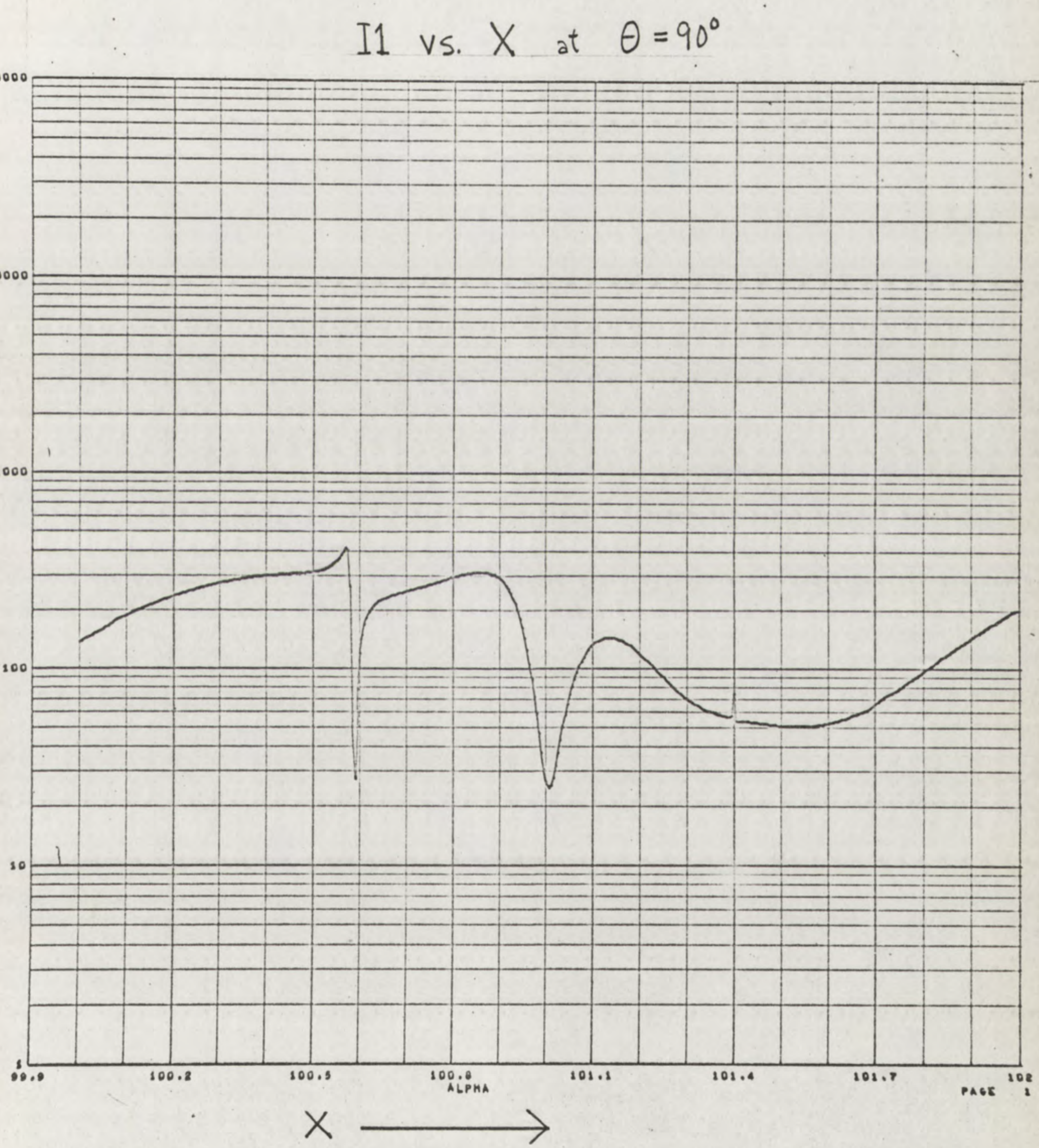

I1 vs. X at $\theta = 90°$
100000
10000
1000
100
10
1
I1
99.9
100.2
100.5
100.8
101.1
101.4
101.7
102
ALPHA
PAGE 1
X

Graph #6b

I2 vs. X at $\theta=90°$

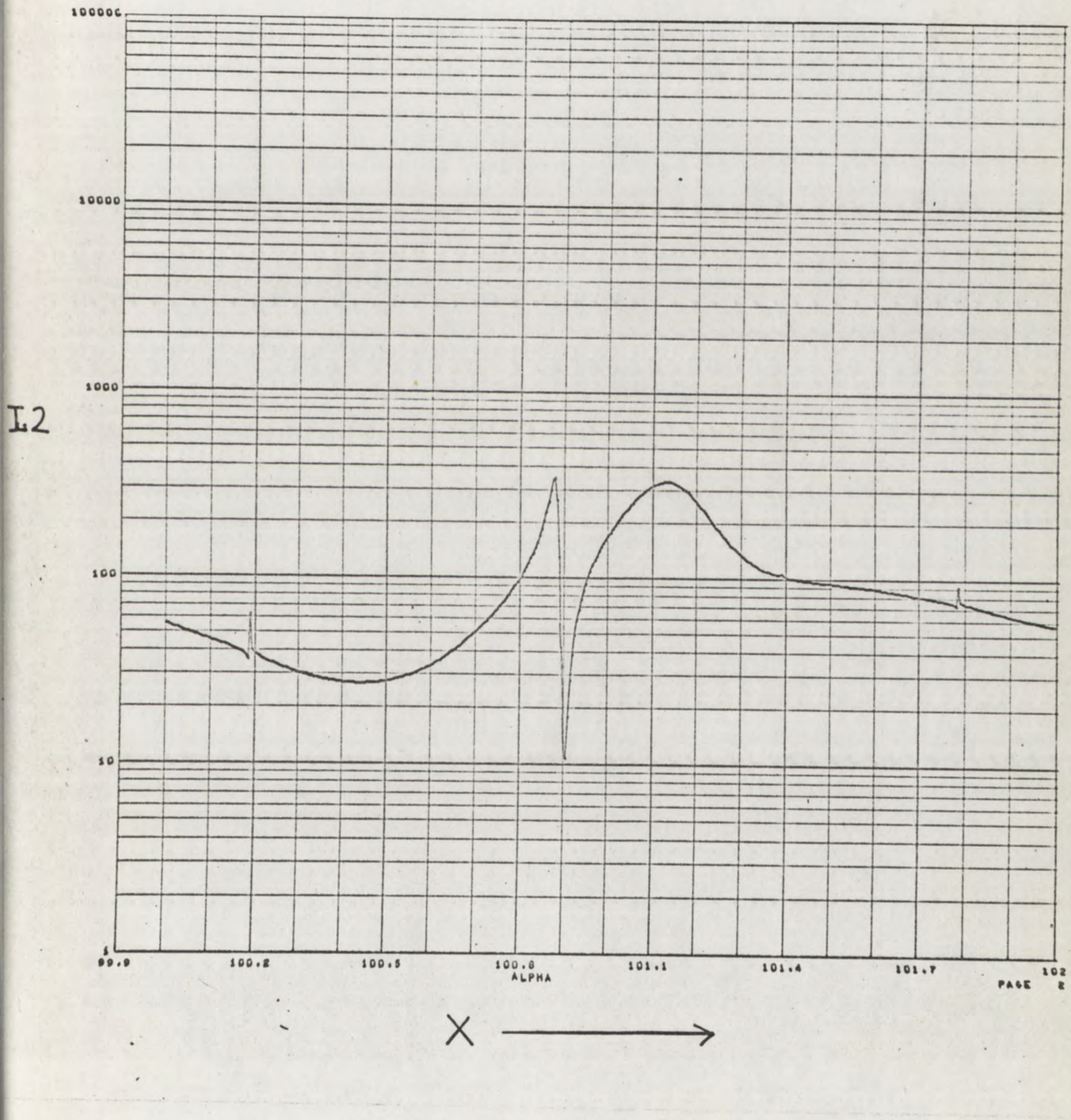

Graph #5 are absent. For this reason it is felt that scattering at 180° is due to a special mechanism that does not affect scattering at most other angles.

The drop sizes for which the previous calculations were made, were large enough to permit the use of ray optics to describe the scattering process. That is, when the drop size is large compared to the wave length of the light, the paths of individual rays can be followed as they are refracted and reflected at the surface of the drop.[21] Sometimes it is quite difficult to determine which ray or bundle of rays makes the major contribution to the intensity of the scattered light in a given angular direction. A method for locating the important rays is discussed by Van de Hulst.[22] It is called the "Localization Principle."

Van de Hulst states that it is possible to locate or "localize" important rays by noting the correspondence between the order, n, of the terms of the series representing $I1$ and $I2$ and a ray striking the sphere with an impact parameter, b, where

5-2 $$b = \frac{\lambda(n + 1/2)}{2\pi}$$

---

[21] See Figure #3.

[22] Van de Hulst, op. cit., p. 208.

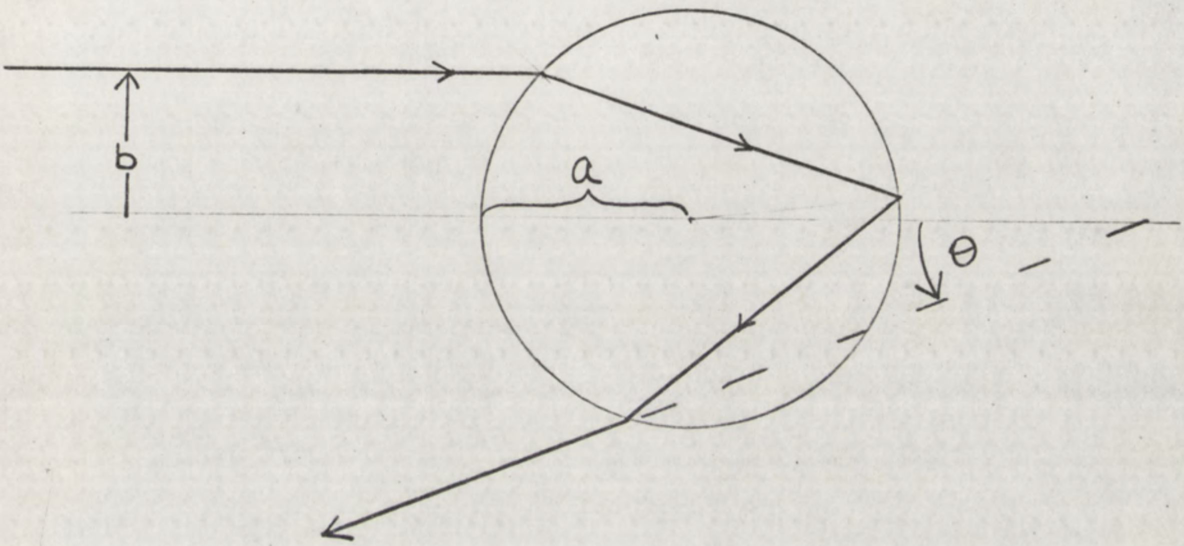

Figure 3.

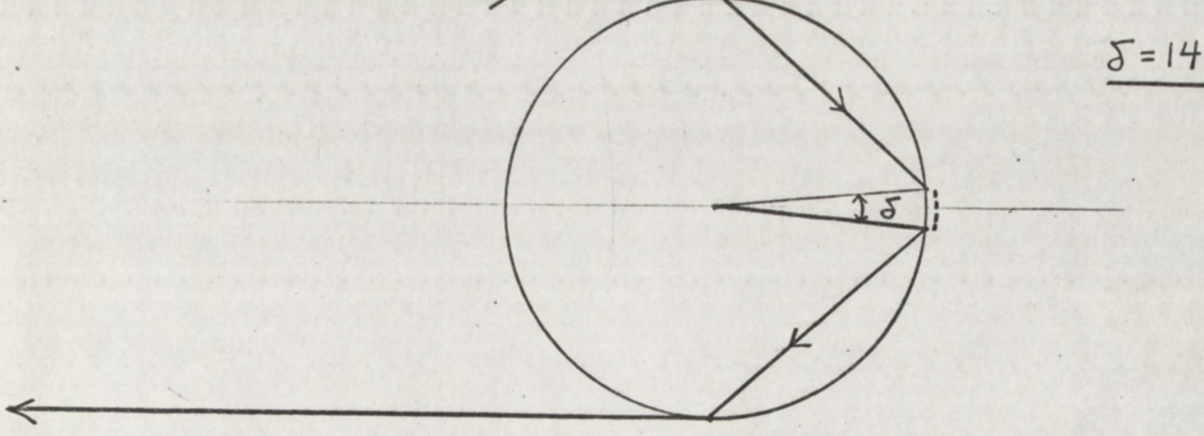

Figure 4.

Letting $I1(N)$ represent the partial sum

$$I1(N) = \left| \sum_{n=1}^{N} \frac{2n+1}{n(n+1)} \left(a_n \pi_n + b_n \tau_n \right) \right|^2,$$

a plot of $I1(N)$ vs. N would show the growth of $I1(N)$ as each additional term is added. It will be a curve showing the contribution of each term in the series and therefore indicating the relative contribution of the associated ray. Large jumps in $I1(N)$ that are not quickly canceled out by the following terms, correspond to contributing rays at the impact parameter, b, given by equation 5-1.

Debye showed that the amplitudes of the terms of these series fall off sharply for $n+\frac{1}{2} > \chi$.[23] This is consistent with the "Localization Principle," since by equation 5-1 such χ values correspond to impact parameters greater than the drop radius, i.e., rays that do not strike the drop.

Calculations were made, showing the growth of $I1$ as a function of N. These were done for $\chi=500.235$ at different angles to determine if the backscattering angle ($\theta = 180°$) was unique. Graphs #7 through #11 show the results of calculations made at $\theta = 0°, 30°, 90°, 150°, 180°$ respectively. All angles except 180° show contributing rays at many different impact parameters between zero and the drop radius. At 180° this is not the case. Instead, the graph indicates a strong axial ray contribution ($b \approx 0$) and a second ray at b approximately equal to a. Between these extremes the average

---

[23] P. Debye, <u>Annalen der Physik</u>, volumn 30, 1909, p.59.

Graph #7.

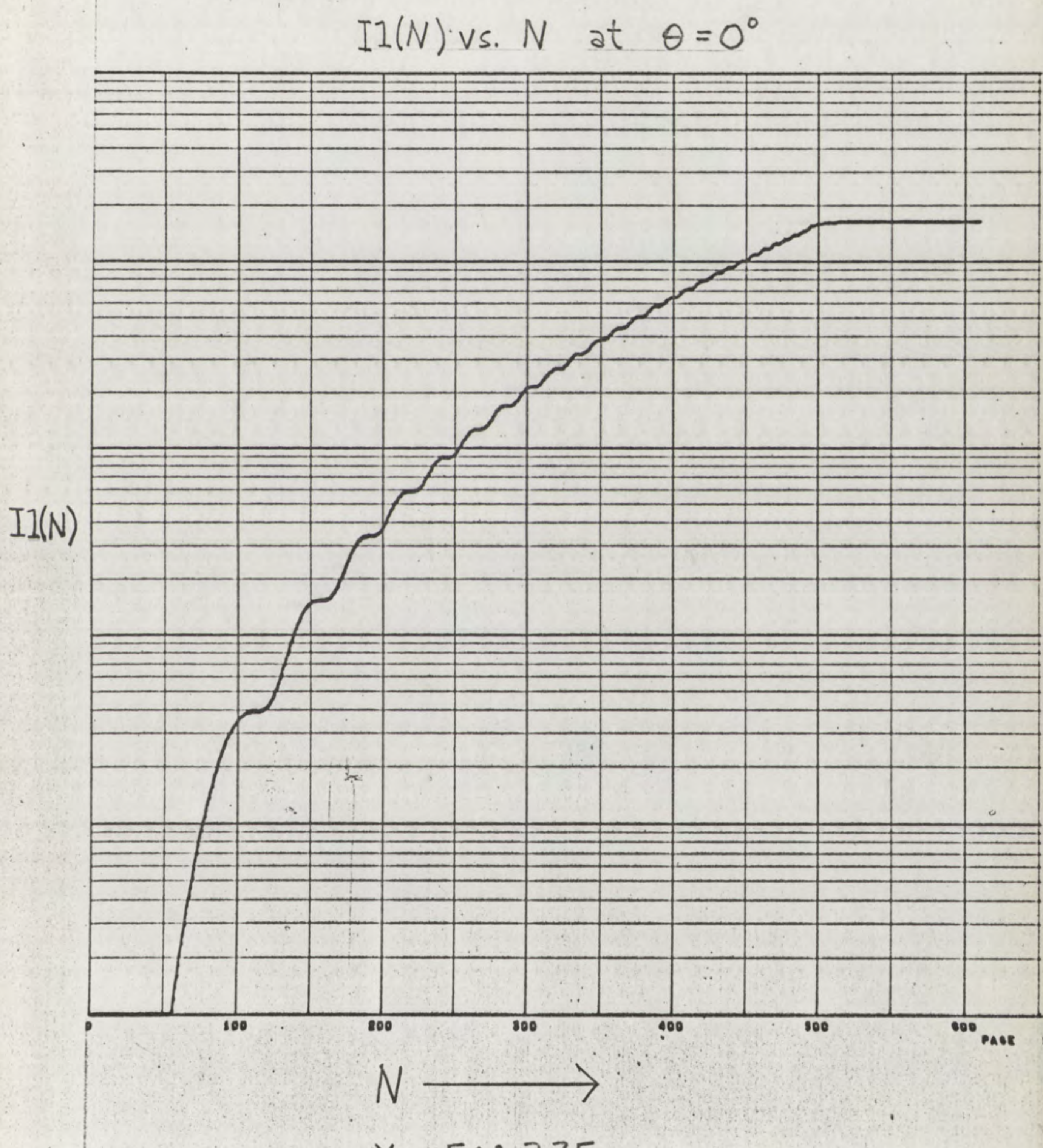

X = 500.235

Graph #8.

I1(N) vs. N at θ = 30°

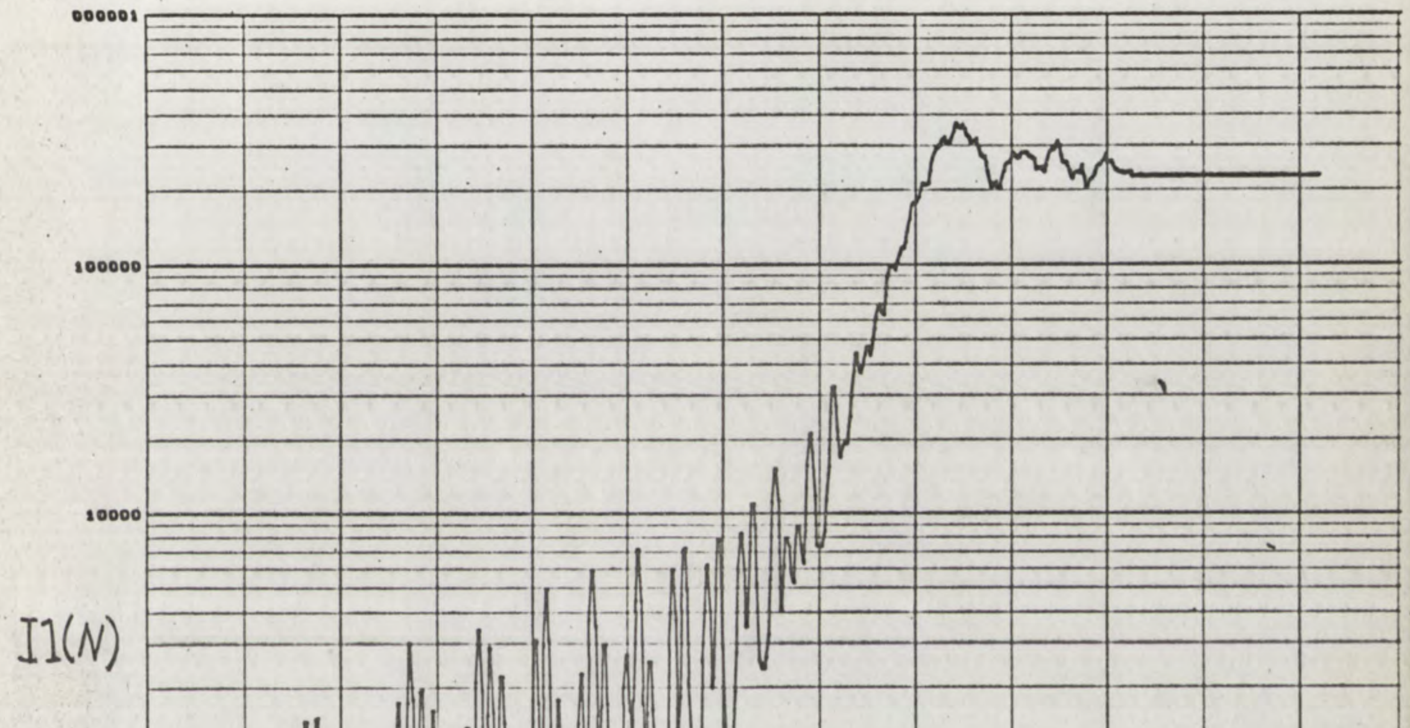

X = 500.235

Graph #9.

I1(N) vs N at $\Theta = 90°$

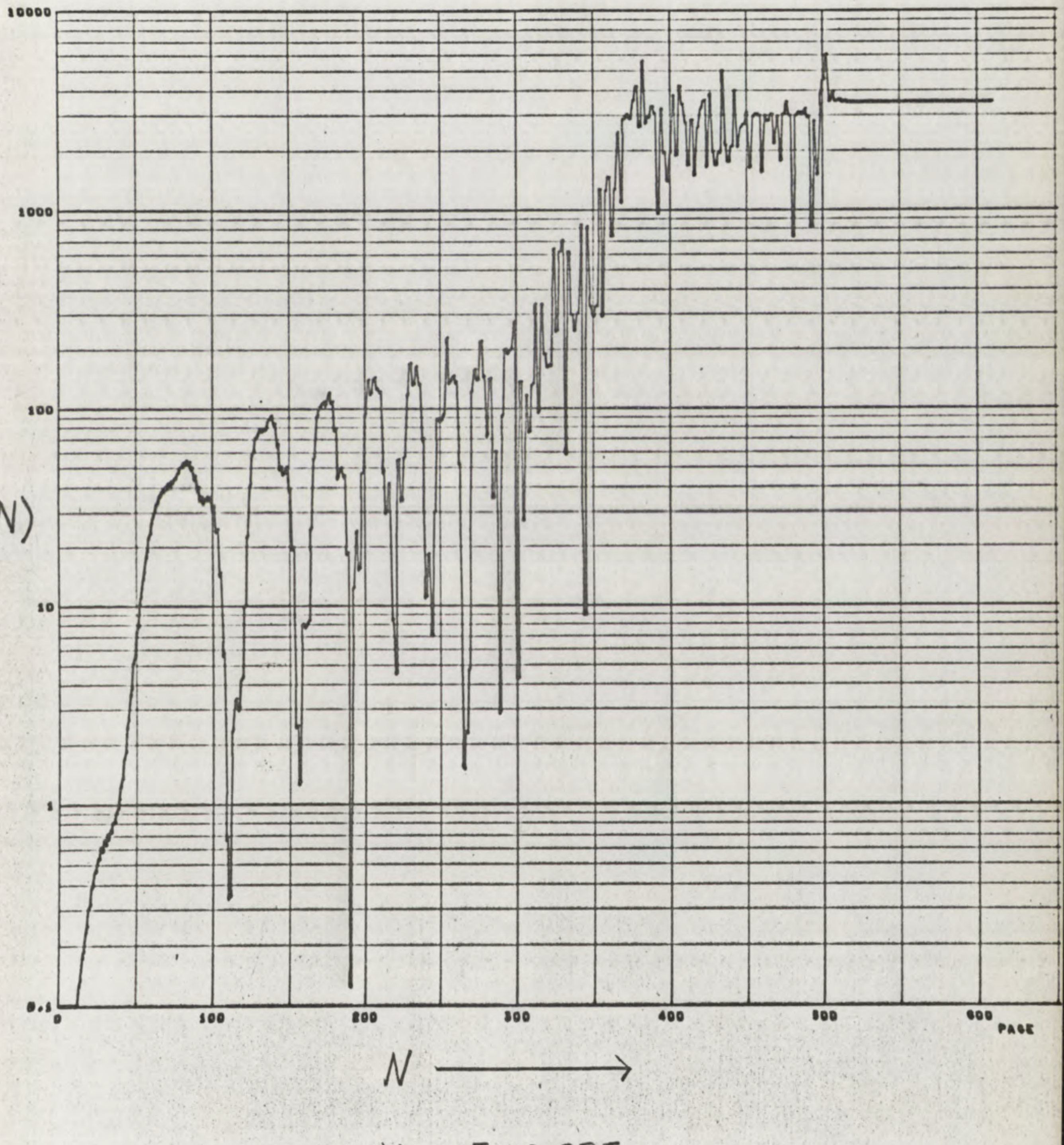

X = 500.235

Graph #10.

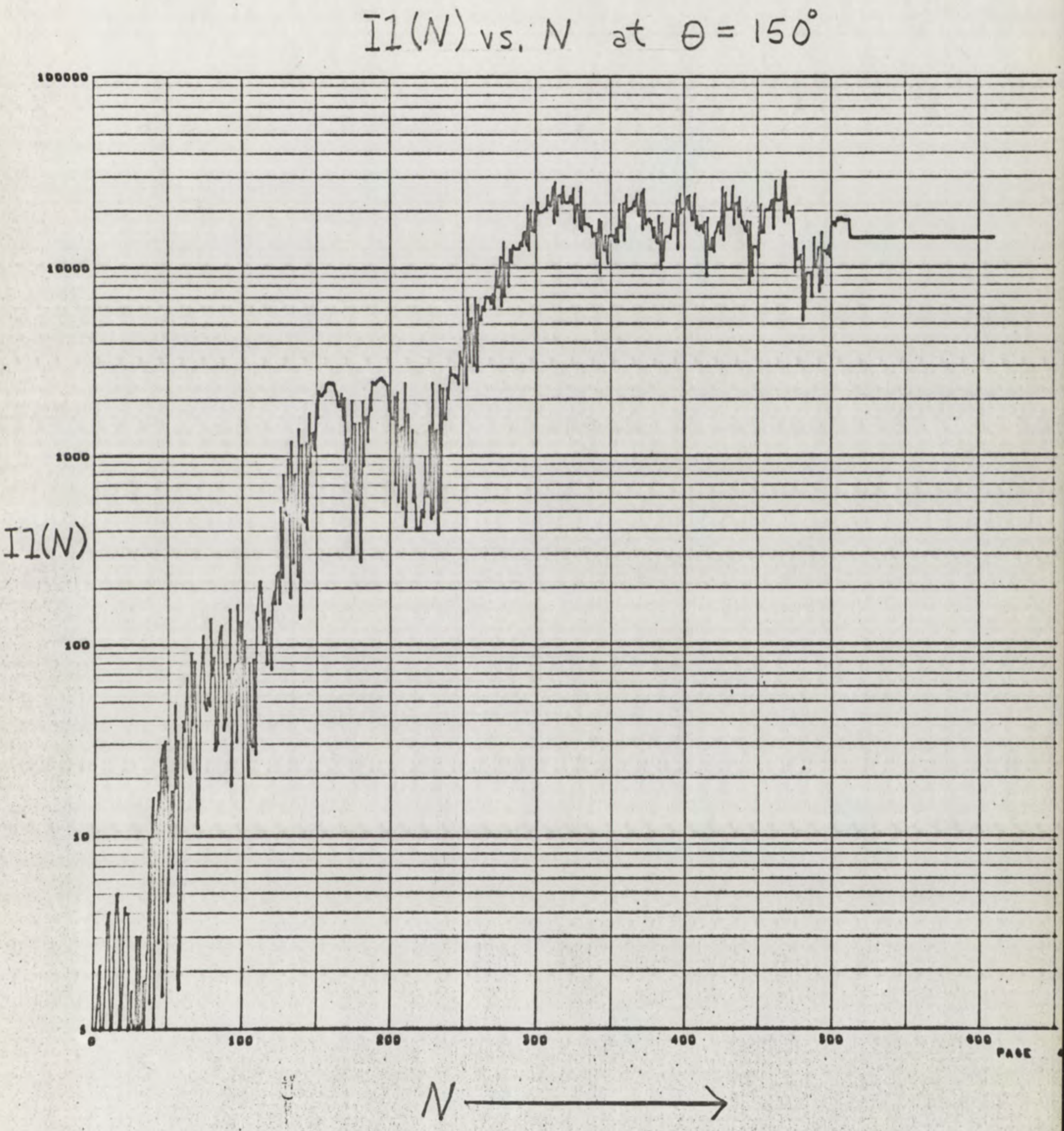

X = 500.235

Graph # 11.

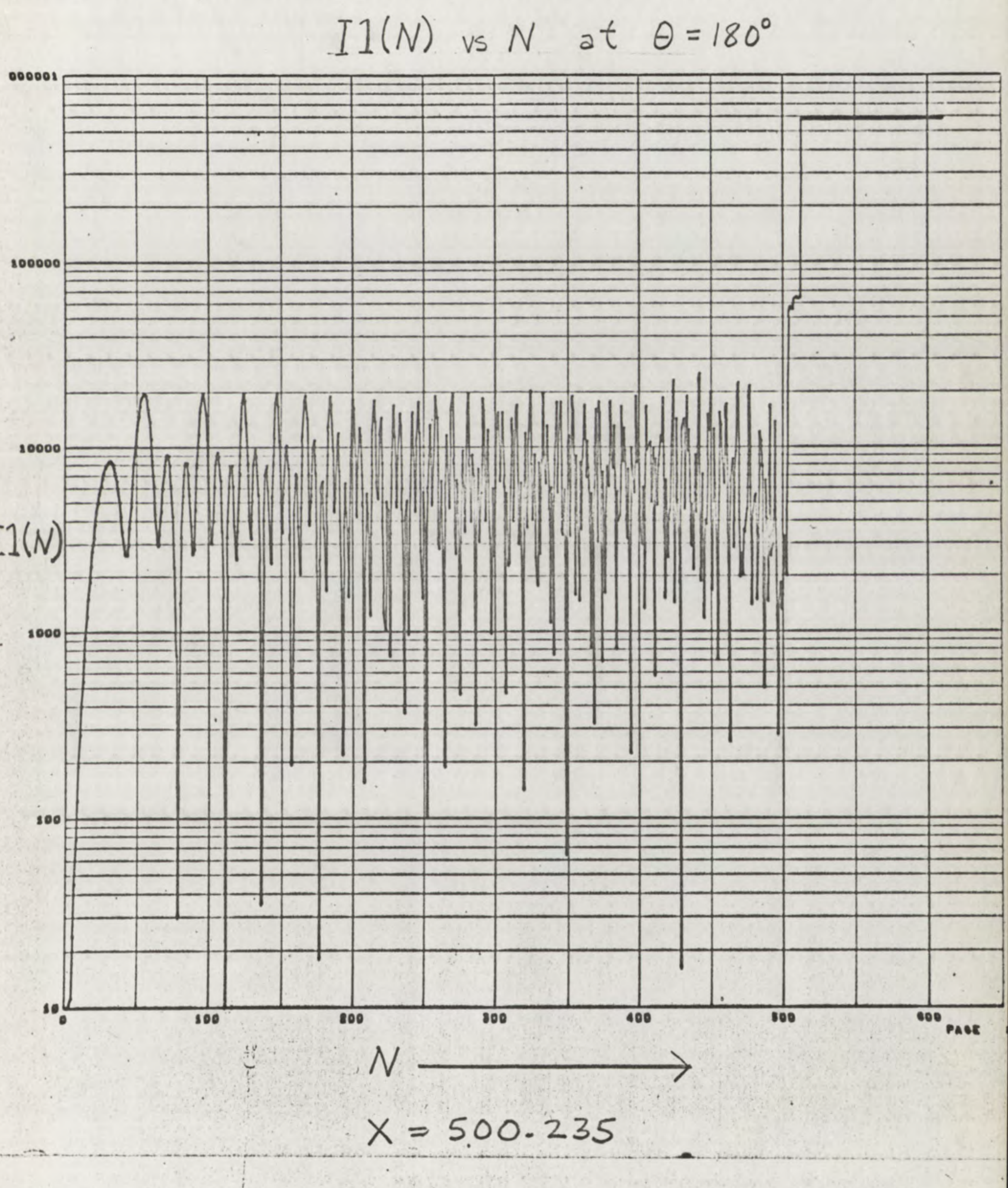

I1(N) vs N at θ = 180°
000001
100000
10000
I1(N)
1000
100
10
0
100
200
300
400
500
600
PAGE
N
X = 500-235

contribution is nil. Thus, the "Localization Principle" has indicated only these two rays as the primary contributors to backscattering. Calculations done by Bryant show that the axial ray's contribution to backscattering, although finite, can not account for the very high values of $I1$ and $I2$ at $180°$.[24]

An attempt to follow the grazing ray (with impact parameter $b = a$), using geometrical optics yields Figure #4. Geometrical optics cannot describe the deflection of this ray through $180°$, for $m = 4/3$. If in some way the ray could travel along the $14°$ of the sphere's surface that separate the incoming and outgoing rays, then the grazing ray could contribute to backscattering.

Van de Hulst suggests that light incident at $b = a$ could travel along the surface of the drop, completing either a fraction of revolution or many revolutions.[25] Light traveling along the surface in this way is referred to as a "surface wave." It is believed that these waves make the major contribution to backscattering from water droplets, i.e., glory.

To see whether the surface wave's contribution is responsible for the actual shape of the $I1$ vs χ curve, the growth of $I1$ as a function of N was calculated for various

---

[24]Howard C. Bryant, Private Communication, 1965.

[25]Van De Hulst, <u>op. cit</u>., p. 365.

χ values. Calculations were made for $\chi =$ 100.515, 100.575, 100.645 and 100.715. Graphs #12 through #15 show the results. Clearly, the surface wave's contribution to the backscattered intensity accounts almost entirely for the shape of the I1 vs. χ curve (Graph #5). This is apparent from the fact that the last few terms of the intensity series cause the final value, I1, to depart greatly from the value it would have if such terms were omitted. These are the terms that correspond to the surface wave's contribution. Without them, I1 would lose most of its characteristic χ dependence at $\chi = 180^\circ$ and the very high intensity peaks would be absent. Therefore surface waves appear to be the primary mechanism for high intensity backscattering of light.

Graph # 12.

I1(N) vs. N at X = 100.515

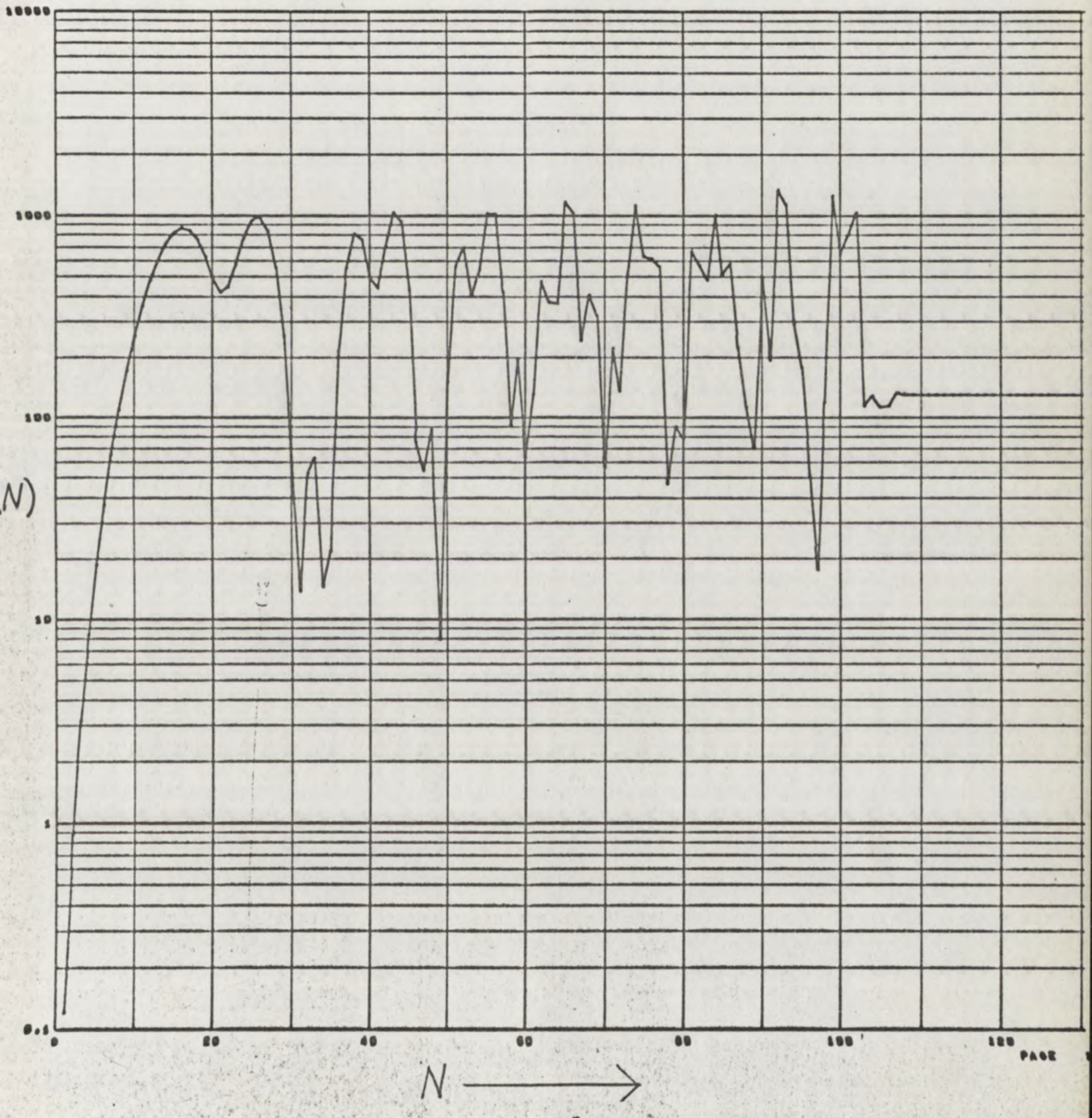

Graph # 13.

I1(N) vs. N at X = 100.575

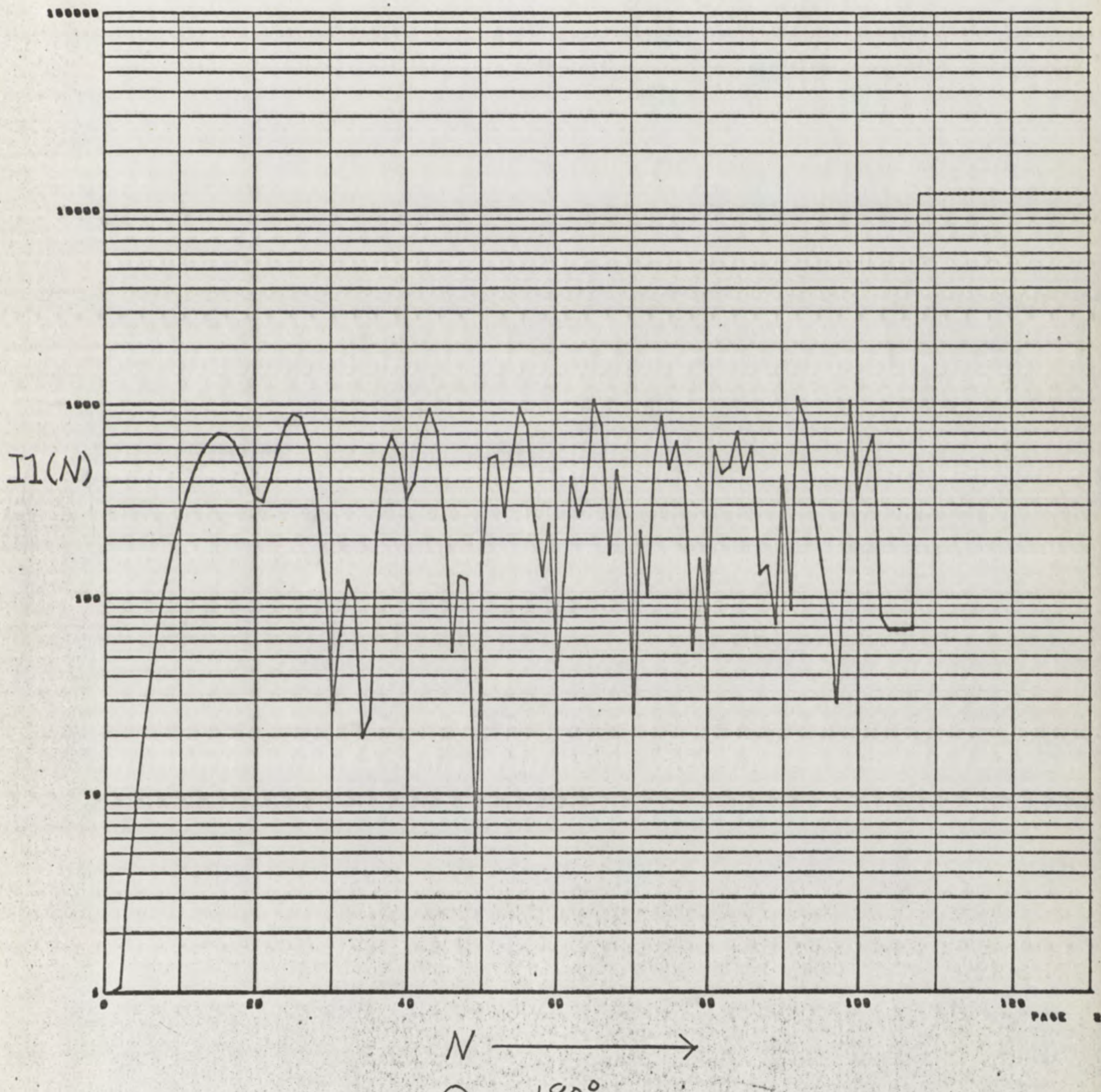

$\Theta = 180°$

Graph #14.

I1(N) vs. N at X = 100.645

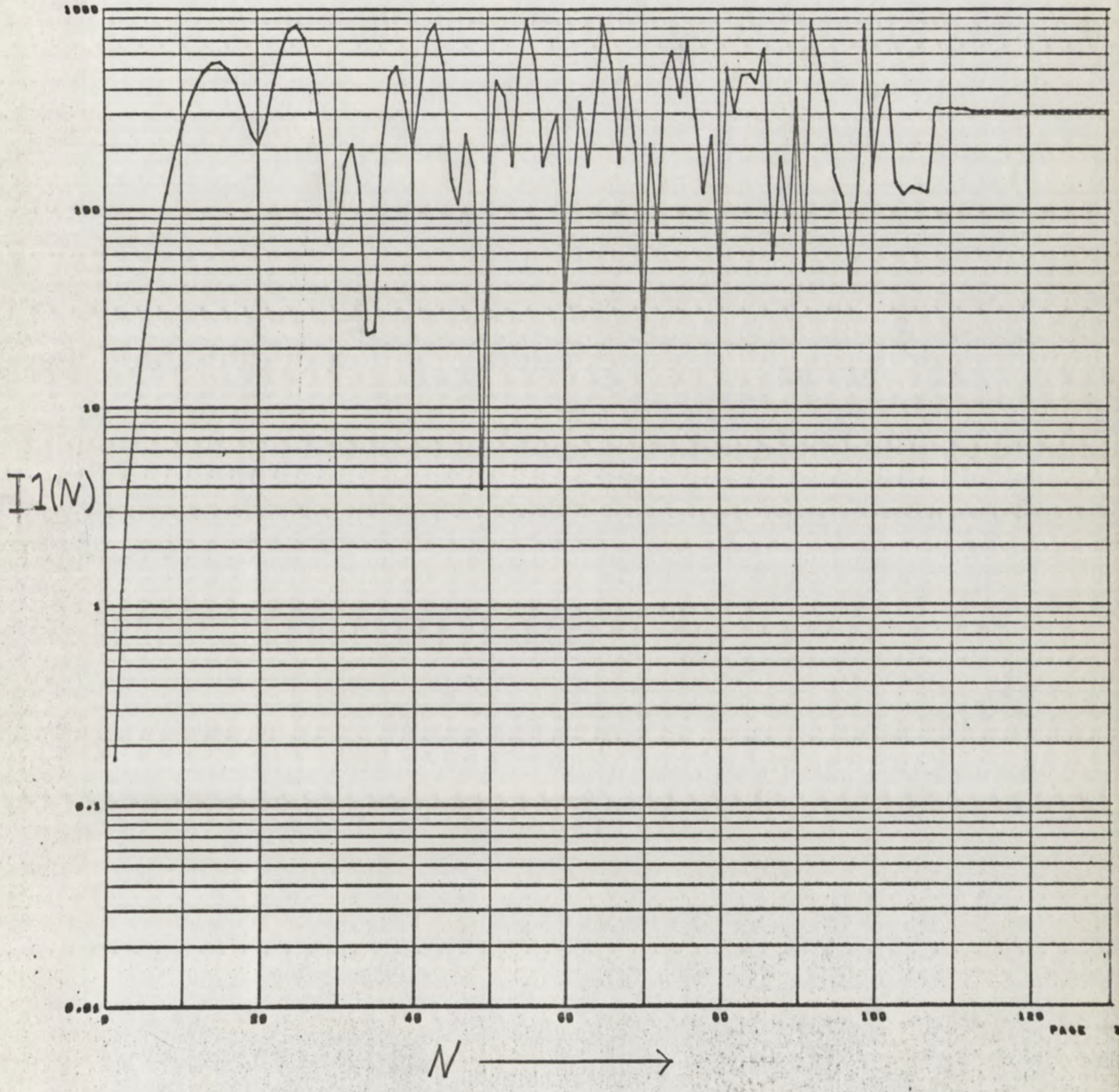

$\theta = 180°$

Graph #15.

I1(N) vs. N at X = 100.715

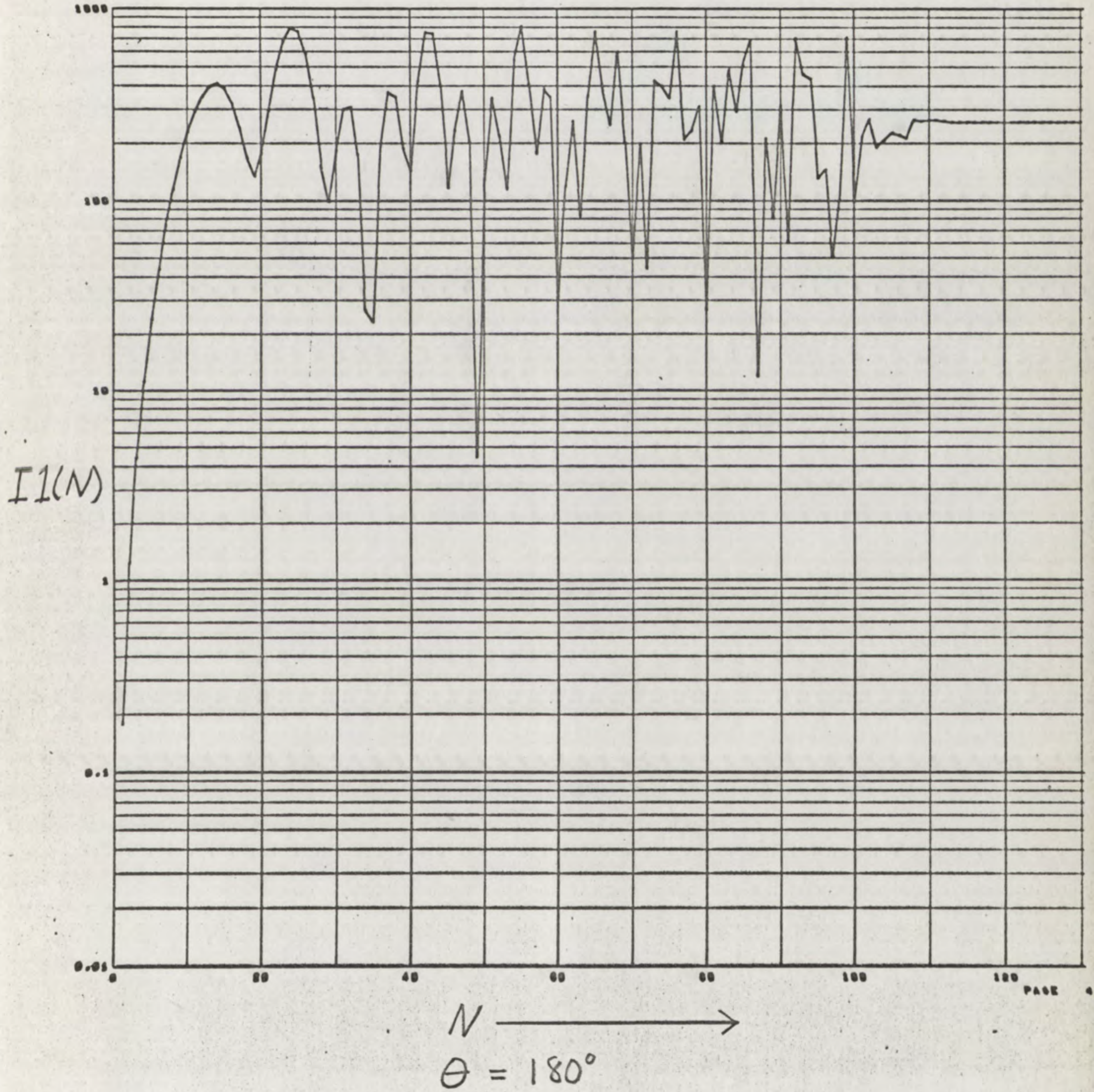

CONCLUSION

In conclusion, three points seem significant. First, this highly detailed study of the intensity functions has revealed the extremely complex structure of their dependence, a fact passed over by other writers. Second, the "Localization Principle" has actually been employed, with meaningful results. Other such uses of this concept are unknown to this writer. Finally, surface waves have been shown to be the primary mechanism for the backscattering of light from water droplets.

APPENDIX I

(1) Given: curl $\vec{H} = \frac{4\pi\vec{I}}{c} + \frac{1}{c}\frac{d\vec{D}}{dt}$

and $\vec{D} = \varepsilon\vec{E}$, $\vec{I} = \sigma\vec{E}$

We can obtain on substitution

$$\text{curl } \vec{H} = \frac{4\pi\sigma\vec{E}}{c} + \frac{\varepsilon}{c}\frac{d\vec{E}}{dt}$$

and if $E = E_0 e^{i\omega t}$ then we have

$$\text{curl } \vec{H} = \frac{4\pi\sigma\vec{E}}{c} + \frac{i\omega\varepsilon\vec{E}}{c} \quad \text{or}$$

$$\text{curl } \vec{H} = i\frac{\omega}{c}\vec{E}\left(\varepsilon - \frac{4\pi\sigma i}{\omega}\right)$$

So we finally have

$$\text{curl } \vec{H} = ikm^2\vec{E}$$

where $k = \frac{\omega}{c}$, $m^2 = \left(\varepsilon - \frac{4\pi\sigma i}{\omega}\right)$

(2) Given: curl $\vec{E} = -\frac{1}{c}\frac{\partial\vec{H}}{\partial t}$ and $\vec{H} = H_0 e^{i\omega t}$

we have curl $\vec{E} = -\frac{i\omega\vec{H}}{c}$ or

$$\text{curl } \vec{E} = -ik\vec{H} \quad \text{where } k = \frac{\omega}{c}$$

APPENDIX II

Given: curl $\vec{H} = i k m^2 \vec{E}$ (a)

curl $\vec{E} = -i k \vec{H}$ (b)

Substituting (b) into (a) we have curl curl $\vec{E} = k^2 m^2 \vec{E}$.

using the vector relation

curl curl $\vec{F}$ = grad div $\vec{F} - \nabla^2 \vec{F}$

and by equation 3-11 we have $\operatorname{div} \vec{E} = 0$ so

curl curl $\vec{E} = -\nabla^2 \vec{E}$ and thus we have

$$\nabla^2 \vec{E} + k^2 m^2 \vec{E} = 0$$ vector wave equation

Similarly, substituting (a) into (b) we have

curl curl $\vec{H} = k^2 m^2 \vec{H}$ and this gives

$\nabla^2 \vec{H} - \operatorname{grad} \operatorname{div} \vec{H} + k^2 m^2 \vec{H} = 0$ but by equation 3-20

$\operatorname{div} \vec{H} = 0$ so we have

$$\nabla^2 \vec{H} + k^2 m^2 \vec{H} = 0$$

Thus both $\vec{H}$ and $\vec{E}$ satisfy the vector wave equation of the form

$$\nabla^2 \vec{A} + k^2 m^2 \vec{A} = 0$$

APPENDIX III

Given: ψ — satisfies the scalar wave equation

$$\nabla^2\psi + m^2k^2\psi = 0 \qquad \text{and then}$$

$\vec{M}_\psi$ and $\vec{N}_\psi$ satisfy the vector wave equation.

If u, v are two functions that satisfy the scalar wave equation and $\vec{M}_u$, $\vec{M}_v$, $\vec{N}_u$, $\vec{N}_v$ are the derived vector fields then show that

$$\vec{E} = \vec{M}_v + i\vec{N}_u$$

$$\vec{H} = m(-\vec{M}_u + i\vec{N}_v)$$

are suitable forms for the electric and magnetic vectors, i.e., they satisfy Maxwell's equations.

We know the derived fields have the following properties:

$$\vec{M}_\psi = \mathrm{curl}\,(\vec{r}\psi)$$

$$mk\vec{N}_\psi = \mathrm{curl}\,(\vec{M}_\psi)$$

$$mk\vec{M}_\psi = \mathrm{curl}\,\vec{N}_\psi$$

So we take curl of $\vec{H}$

$$\mathrm{curl}\,\vec{H} = -m\,\mathrm{curl}\,\vec{M}_u + im\,\mathrm{curl}\,\vec{N}_v = -m^2k\vec{N}_u + im^2k\vec{M}_v$$

thus $\quad \mathrm{curl}\,\vec{H} = im^2k\vec{E} \qquad$ Maxwell's Equation

$$\mathrm{curl}\,\vec{E} = \mathrm{curl}\,\vec{M}_v + i\,\mathrm{curl}\,\vec{N}_u = mk\vec{N}_v + imk\vec{M}_u$$

thus $\quad \mathrm{curl}\,\vec{E} = -ik\vec{H}$

$$E_\theta = \frac{1}{r\sin\theta}\frac{\partial(rv)}{\partial\phi} + \frac{i}{mkr}\frac{\partial^2(ru)}{\partial r\partial\theta}$$

$$\frac{\partial(rv)}{\partial\phi} = \frac{-i}{k}e^{-ikr+i\omega t}\cos\phi\sum_{n=1}^{\infty} b_n\frac{2n+1}{n(n+1)}P_n^1(\cos\theta)$$

$$\frac{\partial^2(ru)}{\partial r\partial\theta} = -e^{-ikr+i\omega t}\cos\phi\sum_{n=1}^{\infty} a_n\frac{2n+1}{n(n+1)}\frac{dP_n^1(\cos\theta)}{d\theta}$$

$m=1$ outside

$$E_\theta = \frac{-i\cos\phi}{kr}e^{-ikr+i\omega t}\left\{\sum_{n=1}^{\infty}\frac{2n+1}{n(n+1)}\left(a_n\frac{dP_n^1(\cos\theta)}{d\theta} + \frac{b_nP_n^1(\cos\theta)}{\sin\theta}\right)\right\}$$

$$E_\phi = -\frac{1}{r}\frac{\partial(rv)}{\partial\theta} + \frac{i}{mkr\sin\theta}\frac{\partial^2(ru)}{\partial r\partial\phi}$$

$$\frac{\partial(rv)}{\partial\theta} = \frac{-i\,e^{-ikr+i\omega t}}{k}\sin\phi\sum_{n=1}^{\infty} b_n\frac{2n+1}{n(n+1)}\frac{dP_n^1(\cos\theta)}{d\theta}$$

$$\frac{\partial^2(ru)}{\partial r\partial\phi} = e^{-ikr+i\omega t}\sin\phi\sum_{n=1}^{\infty} a_n\frac{2n+1}{n(n+1)}P_n^1(\cos\theta)$$

$$E_\phi = \frac{i}{kr}\sin\phi\, e^{-ikr+i\omega t}\sum_{n=1}^{\infty}\frac{2n+1}{n(n+1)}\left\{a_n\frac{P_n^1(\cos\theta)}{\sin\theta} + b_n\frac{dP_n^1(\cos\theta)}{d\theta}\right\}$$

BIBLIOGRAPHY

Boll, Chu, Churchill, Leacock. Tables of Light Scattering Functions. Ann Arbor: University of Michigan Press, 1958.

Born, M. and E. Wolf. Principles of Optics. New York: The Macmillan Company, 1964.

Debye, P. Annalen der Physik. Volumn 30, p. 59, 1909.

Deirmendjian, D. and R.J. Clasen. Light Scattering on Partially Absorbing Homogeneous Spheres of Finite Size. Santa Monica: The Rand Corporation, 1962.

Eisberg, Robert M. Fundamentals of Modern Physics. New York: John Wiley & Sons, 1961.

Gumprecht, R. O. and C.M. Sliepcenich. Light-Scattering Functions for Spherical Particles. Ann Arbor: University of Michigan Press, 1951.

Irving, J. and N. Mullineux. Mathematics in Physics and Engineering. New York: Academic Press, 1959.

Lowan, A.N. Tables of Scattering Functions for Spherical Particles. Department of Commerce, National Bureau of Standards Applied Mathematics Series Number 4. Washington: Government Printing Office, 1949.

Mie, G. Annalen der Physik. Volumn 25, p. 377, 1908.

Morse, P.M. and H. Feshbach. Methods of Theoretical Physics. New York: McGraw-Hill Company, 1953.

Penndorf, B. and B. Goldberg. New Tables of Mie Scattering Functions for Spherical Particles. Geophysical Research Papers Number 45. Geophysics Research Directorate, Air Force Cambridge Research Center, Air Research and Development Command, 1956.

Shiff, I.S. Quantum Mechanics. New York: McGraw-Hill Company, 1955.

Slater, J.C. and N.H. Frank. <u>Electromagnetism</u>. New York: McGraw-Hill Company, 1947.

Stratton, J.A. <u>Electromagnetic Theory</u>. New York: McGraw-Hill Company, 1941.

Van de Hulst, H.C. <u>Light Scattering by Small Particles</u>. New York: John Wiley & Sons, 1957.